Contribution from the Department of Chemistry,
University of Wisconsin—Madison, Madison, Wisconsin 53706

Synthesis, Stereochemistry, and Bonding of the Cobalt–Cobalt Multiple-Bonded (Pentamethylcyclopentadienyl)- and Cyclopentadienylcobalt Carbonyl Dimers, $[Co_2(\eta^5\text{-}C_5R_5)_2(\mu\text{-}CO)_2]^n$ (R = Me, n = 0, 1–; R = H, n = 1–): A Comparative Analysis of the Antibonding Dimetal Nature of the Unpaired Electron in the Monoanions and Its Structural Effects upon Oxidation

LARRY M. CIRJAK, ROBERT E. GINSBURG, and LAWRENCE F. DAHL*

Received September 2, 1980; Revised Manuscript Received September 18, 1981

The preparation, properties, structure, and resulting bonding implications of the (pentamethylcyclopentadienyl)cobalt carbonyl neutral dimer, $[Co_2(\eta^5\text{-}C_5Me_5)_2(\mu\text{-}CO)_2]^n$ (n = 0), and its paramagnetic monoanion (n = 1–) as the $[Na(2,2,2\text{-crypt})]^+$ salt are reported together with the corresponding cyclopentadienyl $[Co_2(\eta^5\text{-}C_5H_5)_2(\mu\text{-}CO)_2]^-$ monoanion as the tetraphenylarsonium salt. Distinct geometrical differences are found among the solid-state structures of the neutral dimer and both monoanions. The entire molecular configuration of the neutral dimer closely conforms to C_{2v}-$m2m$ symmetry with the two eclipsed, almost parallel C_5Me_5 rings being essentially perpendicular to the nearly planar $Co_2(CO)_2$ core, which is puckered by only 4–5° from planarity. In contrast, the C_5Me_5-containing monoanion exhibits the following marked geometrical distortions: (1) its $Co_2(CO)_2$ core is significantly puckered by 10–12° from planarity; (2) the two C_5Me_5 rings are twisted from an eclipsed conformation and inclined by 26.5° from being coparallel; (3) one of the two bridging carbonyl ligands possesses extremely large out-of-plane thermal ellipsoids indicative of an averaged structure in which this one bridging carbonyl occupies at least two bent orientations in the crystalline state. The fact that the corresponding electronically equivalent C_5H_5-containing monoanion (of crystallographic C_i-$\bar{1}$ site symmetry) experimentally conforms to a C_{2h}-$2/m$ geometry consisting of a planar D_{2h} $Co_2(CO)_2$ core with perpendicular C_5H_5 ligands points to steric effects being responsible for the considerable distortion of the C_5Me_5-containing monoanion from an analogous geometry. Despite these geometrical differences, the corresponding Co–Co and Co–CO bond lengths (for the well-behaved bridging carbonyl) in the C_5Me_5-containing monoanion are only 0.008 and 0.012 Å longer, respectively, than those in the C_5H_5-containing monoanion. Salient structural differences between the two members of the $[Co_2(C_5Me_5)_2(\mu\text{-}CO)_2]^n$ series (n = 0, 1–) are completely consistent with the Pinhas–Hoffmann energy-level ordering diagram, which for each monoanion places the unpaired electron in a HOMO (of b_2 representation under C_{2v} symmetry) composed mainly of out-of-plane antibonding π^* dimetal symmetry orbital character. In the C_5Me_5-containing monoanion, the Co–Co and Co–CO bond lengths are 2.372 (1) and 1.827 Å (average of 1.820 (6) and 1.834 (6) Å), respectively, while the corresponding bond lengths in its oxidized neutral dimer are 2.338 (2) and 1.851 Å (average of four values in the range 1.841 (12)–1.860 (12) Å), respectively. Hence, removal of an electron from the monoanion results in a *shortening* of the Co–Co distance by 0.034 Å and a concomitant *lengthening* of the mean Co–CO bond length by 0.024 Å. The much smaller observed decrease in the Co–Co bond length relative to that of 0.08 Å predicted by Pinhas and Hoffmann from quantum-mechanical calculations may be readily ascribed to the simultaneous *increase* in the lengths of the Co–CO bonds (upon oxidation of the monoanion), which in being much stronger than the Co–Co interactions are the dominant factor in opposing any decrease in the Co–Co distance. The fact that the imposed symmetry of the HOMO (b_2) precludes any carbonyl orbital character for a planar $Co_2(CO)_2$ core points to the observed increase in the Co–CO bond lengths being an indirect consequence of the loss of negative charge, which in turn lowers the metal AO's relative to the π^*(CO) symmetry orbitals (SO's) and thereby decreases the d_π(Co) → π^*(CO) back-bonding; this charge effect is also in harmony with the IR carbonyl frequency of 1670 cm^{-1} for the monoanion in THF solution being 80 cm^{-1} less than that of 1750 cm^{-1} for the neutral dimer in THF solution. Additional bond length evidence that the LUMO in the neutral dimer and HOMO in its reduced monoanion is the out-of-plane MO (b_2), which from energetic considerations must have considerable $[d_{yz}(Co)\text{–}e_1^-(Cp\ ring)]^*$ antibonding character, has been uncovered from the distinct geometrical variations in the corresponding Co–C_5Me_5(ring) and C(ring)–C(ring) distances between the neutral $Co_2(\eta^5\text{-}C_5Me_5)_2(\mu\text{-}CO)_2$ dimer and the previously analyzed $Co(\eta^5\text{-}C_5Me_5)(CO)_2$ molecule.

Introduction

Our research in the field of the $M_2(\eta^5\text{-}C_5R_5)_2(\mu\text{-}X)_2$-type dimers (where X = CO, NO) commenced with metal cluster chemistry involving the reduction of cyclopentadienylcobalt dicarbonyl, from which the $[Co_2(\eta^5\text{-}C_5H_5)_2(\mu\text{-}CO)_2]^-$ monoanion was isolated and stereochemically characterized by Ginsburg and Dahl[1] from IR and ESR measurements in solution and from an X-ray diffraction study in the solid state as the $[AsPh_4]^+$ salt (**1a**). While this work was being written up, Schore, Ilenda, and Bergman[2] reported the analogous preparation and physicochemical properties of this same binuclear cobalt radical anion including an X-ray investigation of its bis(triphenylphosphine)iminium salt (**1b**). They also showed that this paramagnetic monoanion could be reversibly oxidized to the corresponding neutral dimer (**2**). Lee and Brintzinger[3] independently isolated the neutral dimer as one of the products of the photolysis of $Co(\eta^5\text{-}C_5H_5)(CO)_2$ at low temperature under a N_2-swept atmosphere. This $[Co_2(\eta^5\text{-}C_5H_5)_2(\mu\text{-}CO)_2]^n$ series (n = 0, 1–) stimulated considerable activity not only in terms of its chemical utility (Figure 1), which was demonstrated both by Bergman and co-workers[4] and by Lee and Brintzinger,[5] but also from a theoretical viewpoint in that the monoanion and its neutral parent correspond from the EAN rule to a predicted metal–metal bond order (BO) of 1.5 and 2.0, respectively. Since the double-bonded neutral parent is isoelectronic with the corresponding iron cyclopentadienyl nitrosyl dimer, $Fe_2(\eta^5\text{-}C_5H_5)_2(\mu\text{-}NO)_2$,[6]

(1) (a) Ginsburg, R. E. Ph.D. Thesis, University of Wisconsin–Madison, 1978. (b) Ginsburg, R. E.; Dahl, L. F., unpublished results.
(2) (a) Schore, N. E.; Ilenda, C. S.; Bergman, R. G. *J. Am. Chem. Soc.* **1977**, *99*, 1781–1787. (b) Schore, N. E.; Ilenda, C. S.; Bergman, R. G. *Ibid.* **1976**, *98*, 256–258. (c) Ilenda, C. S.; Schore, N. E.; Bergman, R. G. *Ibid.* **1976**, *98*, 255–256.
(3) Lee, W.-S.; Brintzinger, H. H. *J. Organomet. Chem.* **1977**, *127*, 87–92.
(4) Schore, N. E.; Ilenda, C.; Bergman, R. G. *J. Am. Chem. Soc.* **1976**, *98*, 7436–7438.
(5) Lee, W.-S.; Brintzinger, H. H. *J. Organomet. Chem.* **1977**, *127*, 93–103.
(6) Brunner, H. *J. Organomet. Chem.* **1968**, *74*, 173–178.

0020-1669/82/1321-0940$01.25/0

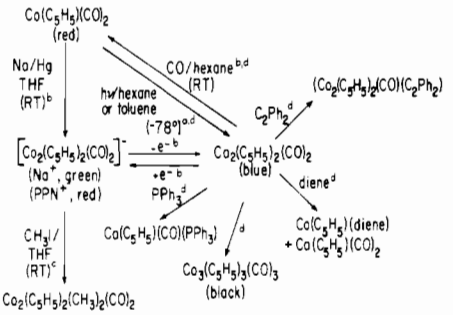

Figure 1. Reaction scheme for the $[Co_2(\eta^5\text{-}C_5H_5)_2(\mu\text{-}CO)_2]^n$ series (n = 0, 1−). Key: a, ref 3; b, ref 2; c, ref 4; d, ref 5.

which was structurally analyzed by Calderôn et al.[7] in 1974, it was of particular interest to us to assess the nature of this multiple-bonded series from an analysis of the change of Co–Co distance with Co–Co bond order. However, attempts by us[1] and others[2,8] to obtain crystals of the oxidized neutral dimer (**2**) in order to carry out an X-ray diffraction study for the purpose of determining the stereochemical consequences due to the removal of the unpaired electron from **1** were not successful. It is noteworthy that the dimer readily decomposes to $Co_3(\eta^5\text{-}C_5H_5)_3(\mu\text{-}CO)_2(\mu_3\text{-}CO)$.[3,9]

On the basis of other work, it was our belief that utilization of pentamethylcyclopentadienyl ligands in place of cyclopentadienyl ligands should significantly alter the redox and solubility properties of the $[Co_2(\eta^5\text{-}C_5H_5)_2(\mu\text{-}CO)_2]^-$ monoanion (**1**). In addition, we presumed that the oxidized neutral dimer would not decompose to the corresponding tricobalt cluster due to the much greater steric requirements of the C_5Me_5 ligands. This speculation led to the subsequent preparation, isolation, and X-ray crystallographic determination of the corresponding dimeric (pentamethylcyclopentadienyl)cobalt monoanion (**3**) by Ginsburg and Dahl[1] as the $[Na(2,2,2\text{-crypt})]^+$ salt (**3a**). The neutral $Co_2(\eta^5\text{-}C_5Me_5)_2(\mu\text{-}CO)_2$ dimer (**4**) was initially obtained and structurally characterized by Cirjak, Ginsburg, and Dahl[1,10] from oxidation of the monoanion; this diamagnetic compound was independently prepared from the thermolysis of $Co(\eta^5\text{-}C_5Me_5)(CO)_2$ and structurally characterized by Cotton, Kaska, and co-workers.[8]

During the course of this work, considerable attention was attracted to the bonding of carbonyl- and nitrosyl-bridged metal cyclopentadienyl dimers by the report of Bernal et al.[11] in 1977 on the X-ray crystallographic investigations of $Co_2(\eta^5\text{-}C_5H_5)_2(\mu\text{-}NO)_2$[12] (Co–Co BO = 1.0) and the paramagnetic $Co_2(\eta^5\text{-}C_5H_5)_2(\mu\text{-}NO)(\mu\text{-}CO)$[13] (Co–Co BO = 1.5), which are both isomorphic and isostructural in the crystalline state with $Fe_2(\eta^5\text{-}C_5H_5)_2(\mu\text{-}NO)_2$ (Fe–Fe BO = 2.0). The near constancy (within 0.01 Å) in the metal–metal bond length of these two cobalt dimers and the dimeric monoanion **1** (Co–Co BO = 1.5) resulted in the conclusion by Bernal et al.[11] that "the successive increase in bond order predicted by the EAN rule is not observed." In turn, these structural studies generated a theoretical molecular orbital examination by Pinhas and Hoffmann[14] in 1979 of the above four dimers together with the nonplanar $Ni_2(\eta^5\text{-}C_5H_5)_2(\mu\text{-}CO)_2$ and planar $Ni_2(\eta^5\text{-}C_5H_4Me)_2(\mu\text{-}CO)_2$ dimers (BO = 1.0), which had been structurally analyzed by Byers and Dahl.[15] From calculated Walsh-type diagrams of $[Co_2(\eta^5\text{-}C_5H_5)_2(\mu\text{-}CO)_2]^n$ (n = 0, 1−, 2−) Pinhas and Hoffmann[14] predicted a Co–Co bond lengthening of 0.13–0.16 Å upon going from a d^8 Co(I)–d^8 Co(I) dimer (for n = 0 with a Co–Co BO = 2.0) to a d^9 Co(0)–d^9 Co(0) dimer (for n = 2− with a Co–Co BO = 1.0). The observed invariance of the Co–Co bond lengths upon a change from BO = 1.5 to BO = 1.0 led to the statement by Pinhas and Hoffmann[14] that "unfortunately, we have no explanation of the discrepancy between the calculated and observed distances".

The gas-phase negative ion chemistry of $Co(\eta^5\text{-}C_5H_5)(CO)_2$ via ion cyclotron resonance spectroscopy was presented in 1977 by Corderman and Beauchamp,[16] who observed the formation of the $[Co_2(\eta^5\text{-}C_5H_5)_2(CO)_2]^-$ monoanion by the reaction of the generated $[Co(\eta^5\text{-}C_5H_5)(CO)]^-$ monoanion with the neutral $Co(\eta^5\text{-}C_5H_5)(CO)_2$ precursor. A low-temperature powder ESR study of the $[Co_2(\eta^5\text{-}C_5H_5)_2(CO)_2]^-$ monoanion, generated by the reduction of $Co(\eta^5\text{-}C_5H_5)(CO)_2$ with a solution of sodium in either THF or HMPA, and the isoelectronic $Co_2(\eta^5\text{-}C_5H_5)_2(\mu\text{-}NO)(\mu\text{-}CO)$ dimer[13] was reported by Symons and Bratt[17] in 1979. Their analysis of the solid-state ESR spectra recorded at 77 K for these two dimeric species, which exhibit similar solution ESR spectra,[2a,11] led to the conclusion that both cobalt atoms in each dimer are identical in the solid state and that the unpaired electron may be in either an in-plane or out-of-plane dicobalt π^*-antibonding orbital having an estimated total 3d Co spin density of ca. 75%.

In 1979 Schore[18] reported the synthesis and spectral characterization of the Na^+–THF salts of four monosubstituted derivatives of the $[Co_2(\eta^5\text{-}C_5H_4R)_2(\mu\text{-}CO)_2]^-$ monoanion (R = $SiMe_3$, $SiMePh_2$, CO_2Me, or CH_2CO_2Me) as well as of the corresponding (pentamethylcyclopentadienyl)cobalt carbonyl monoanion **3** and its oxidized neutral parent **4**. From ESR measurements of the dimeric monoanions at room temperature in THF solutions and at 77 K in glassy 2-methyltetrahydrofuran solutions, Schore[18] proposed from an analysis of the g values that the unpaired electron in each monoanion either occupies the out-of-plane dimetal π^*-antibonding MO given by Pinhas and Hoffmann[14] or an in-plane MO containing dimetal π-bonding orbital character but $[\pi(\text{metal})\text{–}5\sigma(CO)]^*$ antibonding orbital character. Schore[18] pointed out that "on the basis of the experimental evidence available at present a distinction between these two situations does not appear possible".

Presented herein are the full details of our synthesis and physicochemical measurements including X-ray structural determinations of the monoanions of **1** and **3** and of the neutral dimer **4**. An analysis of the determined variations in the Co–Co, Co–CO, and Co–C_5R_5 bond lengths for these dimers (possessing the same metal and bridging ligand atoms) provides convincing evidence (in our minds) not only for the nature of the HOMO containing the unpaired electron in the monoanions but also in accounting for the presumed discrepancy

(7) Calderôn, J. L.; Fontana, S.; Frauendorfer, E.; Day, V. W.; Iske, S. D. A. *J. Organomet. Chem.* **1974**, *64*, C16–18.
(8) Bailey, W. I., Jr.; Collins, D. M.; Cotton, F. A.; Baldwin, J. C.; Kaska, W. C. *J. Organomet. Chem.* **1979**, *165*, 373–381.
(9) (a) King, R. B. *Inorg. Chem.* **1966**, *5*, 2227–2230. (b) Cotton, F. A.; Jamerson, J. D. *J. Am. Chem. Soc.* **1976**, *98*, 1273–1274.
(10) Ginsburg, R. E.; Cirjak, L. M.; Dahl, L. F. *J. Chem. Soc., Chem. Commun.* **1979**, 468–470.
(11) Bernal, I.; Korp, J. D.; Reisner, G. M.; Herrmann, W. A. *J. Organomet. Chem.* **1977**, *139*, 321–336.
(12) Brunner, H. *J. Organomet. Chem.* **1968**, *12*, 517–522.
(13) (a) Müller, J.; Schmitt, S. *J. Organomet. Chem.* **1975**, *97*, C54–56. (b) Herrmann, W. A.; Bernal, I. *Angew. Chem.* **1977**, *89*, 186–187; *Angew. Chem., Int. Ed. Engl.* **1977**, *16*, 172–173.
(14) Pinhas, A. R.; Hoffmann, R. *Inorg. Chem.* **1979**, *18*, 654–658. This work provides a theoretical starting point for a recent comprehensive bonding analysis (Pinhas, A. R.; Albright, T. A.; Hofmann, P.; Hoffmann, R. *Helv. Chim. Acta* **1980**, *63*, 27–49) of a wide variety of known and hypothetical $Rh_2(\eta^5\text{-}C_5H_5)_2(CO)_2X$ complexes (where X includes $Rh(CO)_2^-$, CH_2, CH^n (n = 1−, 1+). $Rh(\eta^5\text{-}C_5H_5)$, and $Rh(\eta^5\text{-}C_5H_5)(CO)$) with carbonyl bridging.
(15) Byers, L. R.; Dahl, L. F. *Inorg. Chem.* **1980**, *19*, 680–692.
(16) Corderman, R. R.; Beauchamp, J. L. *Inorg. Chem.* **1977**, *16*, 3135–3139.
(17) Symons, M. C. R.; Bratt, S. W. *J. Chem. Soc., Dalton Trans.* **1979**, 1739–1743.
(18) Schore, N. E. *J. Organomet. Chem.* **1979**, *173*, 301–316.

between the theoretically calculated and observed metal–metal distances as a function of change in electronic configuration.

Besides our basic objective in obtaining a better understanding of the interrelationship between structure and bonding in these carbonyl-bridged metal dimers, we have also undertaken an investigation of the chemical reactivity of these multiple bonded dimers in forming polynuclear metal clusters. In this connection, our accidental synthesis from the neutral cobalt dimer of the tetranuclear cobalt cluster $Co_4(\eta^5\text{-}C_5Me_5)_2(CO)_4(\mu\text{-}CO)(\mu_3\text{-}CO)_2$[1,19] has led to the development of a rational synthesis for obtaining mixed-metal clusters in reasonable quantities under mild conditions by photogenerated metal-fragment addition across the Co–Co double-bonded neutral dimer (**4**).[20] This designed photochemical procedure has given rise to two electronically equivalent but structurally different series of triangular dicobalt–metal clusters, $MCo_2(\eta^5\text{-}C_5Me_5)_2(\mu\text{-}CO)_3(\mu_3\text{-}CO)$ [where M = $Cr(\eta^6\text{-}C_6H_5Me)$, $Mn(\eta^5\text{-}C_5H_4Me)$, $Fe(\eta^4\text{-}C_4H_4)$] and $MCo_2(\eta^5\text{-}C_5Me_5)_2(\mu\text{-}CO)_2(\mu_3\text{-}CO)$ [where M = $Fe(CO)_3$, $Co(\eta^5\text{-}C_5H_4Me)$].[20]

Experimental Section

Materials and Measurements. All reactions, filtrations, and recrystallizations were carried out under nitrogen with standard Schlenk-type glassware. The following solvents were dried and freshly distilled prior to use: isopropyl alcohol ($CaCl_2$, Mallinckrodt), THF (sodium–benzophenone, Fisher Scientific), hexane (CaH_2, Mallinckrodt), toluene (Na, Fisher Scientific), and diethyl ether (sodium–benzophenone, Mallinckrodt). Pentamethylcyclopentadiene was synthesized by the method of Threlkel and Bercaw.[21] The utilized $Co(\eta^5\text{-}C_5H_5)(CO)_2$ was prepared by the high-pressure reaction of cobaltocene and carbon monoxide,[22a] while $Co(\eta^5\text{-}C_5Me_5)(CO)_2$ was prepared by the method of Rausch and Genetti[22b] from $Co_2(CO)_8$ and C_5Me_5H. Dicobalt octacarbonyl (Strem) and 2,2,2-cryptate (PCR) were used without further purification. The [PPN]Cl, prepared by a literature method,[23a] and Ph_4AsCl (Aldrich) were each dried overnight at 80 °C (10^{-2} torr), prior to use. Anhydrous $FeCl_3$ was prepared by a literature method[23b] and was used without further purification. The neutral alumina used for column chromatography was deactivated with approximately 5.5% water.

Infrared spectra were recorded on a Beckman Model 4240 spectrophotometer. Proton NMR spectra were recorded on a JEOL MH 100-MHz spectrometer; all chemical shifts are reported as ppm downfield from Me_4Si. Mass spectra were run on an AEI MS902C high-resolution mass spectrometer. Electronic spectra were recorded with a Cary 14 spectrometer, while EPR spectra were obtained on a Varian E-3 or E-15 spectrometer. Photolyses were carried out in a Pyrex glass or quartz water-cooled apparatus with radiation supplied from a 450-W Hanovia mercury vapor lamp.

Preparation and Physical Properties of $[M]^+[Co_2(\eta^5\text{-}C_5H_5)_2(\mu\text{-}CO)_2]^-$ (Where M = PPN, $AsPh_4$). The sodium salt of the $[Co_2(\eta^5\text{-}C_5H_5)_2(\mu\text{-}CO)_2]^-$ monoanion was prepared independently by a method similar to that reported by Bergman and co-workers.[2] $Co(\eta^5\text{-}C_5H_5)(CO)_2$ (2 mL, 2.6 g, 14 mmol) was dissolved in 10 mL of THF and added to a stirred suspension of Na sand (0.6 g, 26 mmol) in 10 mL of THF. The mixture was stirred for 8–10 h or until there was no starting material present (as indicated by an infrared spectrum of the THF solution). This reaction produced a slightly soluble green solid formulated as the sodium salt of the $[Co_2(C_5H_5)_2(CO)_2]^-$ monoanion. Precipitation of the green pyrophoric salt was completed by the addition of 15 mL of hexane to the reaction mixture. After settling, the solution was filtered and the residue washed three times with 3:2 (v/v) mixtures of THF/hexane to remove the $NaCo(CO)_4$ (i.e., identified as such by an infrared carbonyl band at 1880 cm^{-1}) produced during reduction. The remaining residue was exhaustively extracted with THF until only the excess Na and an unidentified black solid remained in the flask. Yields of the Na^+ salt averaged 1.0–1.5 g (50–70% yield based on $Co(\eta^5\text{-}C_5H_5)(CO)_2$). Dry THF (30 mL) was added to a known quantity of $[Na]^+[Co_2(\eta^5\text{-}C_5H_5)_2(CO)_2]^-$ and excess [PPN]Cl, and the solution was stirred overnight, filtered, and then concentrated to half the volume of THF under vacuum. The remaining solution was carefully layered with 20–30 mL of dry toluene. Crystalline material precipitated out during the following 24 h. The $[Ph_4As]^+$ salt was made by a layering of a solution of Ph_4AsCl in isopropyl alcohol over a concentrated solution of the sodium salt in THF. Crystals grew at the interface of the two liquids. The crystals were washed with H_2O to remove the NaCl formed and dried with acetone. The $[Ph_4As]^+$ salt is insoluble in most organic solvents, except Me_2SO, and reacts slowly with chlorinated solvents.

Infrared spectra of the $[Ph_4As]^+$ salt exhibited one bridging carbonyl band at 1690 (s) cm^{-1} in THF and at 1670 (s, br) cm^{-1} in Nujol mull. Its paramagnetism was established from solution EPR spectra, which were invariant to either counterion (viz., Na^+, $[PPN]^+$) or solvent (e.g., THF, glyme, acetone, and acetonitrile). A 0.01 M solution of $[PPN]^+[Co_2(\eta^5\text{-}C_5H_5)_2(\mu\text{-}CO)_2]^-$ in THF showed a 15-line spectrum centered at approximately 3200 G with A_{iso} = 45 G and g_{iso} = 2.09. This EPR spectrum is characteristic of a hyperfine interaction of the unpaired electron in the monoanion with two ^{59}Co nuclei (100% abundance, $I = {}^7/_2$).

Preparation and Physical Properties of $[Na(2,2,2\text{-crypt})]^+[Co_2(\eta^5\text{-}C_5Me_5)_2(\mu\text{-}CO)_2]^-$. The dimeric (permethylcyclopentadienyl)cobalt carbonyl monoanion, $[Co_2(\eta^5\text{-}C_5Me_5)_2(\mu\text{-}CO)_2]^-$, was prepared analogously by reaction with $Co(\eta^5\text{-}C_5Me_5)(CO)_2$ (2.0 g, 4 mmol) except that the reduction was completed in 2–3 h. The solution was then decanted from the excess sodium and the solvent removed under vacuum. Washing with Et_2O or 6:1 (v/v) Et_2O/hexane removed the $NaCo(CO)_4$ produced during the reduction of $Co(\eta^5\text{-}C_5Me_5)(CO)_2$. The isolated sodium salt was found to be soluble in a 3:2 (v/v) mixture of the THF/hexane. The yield of the Na^+ salt was generally 0.5–0.6 g (50–60% yield based on $Co(\eta^5\text{-}C_5Me_5)(CO)_2$. The compound is extremely sensitive to trace quantities of O_2 and H_2O, as evidenced by a change in color from red-yellow to bright green upon oxidation. To a stirred solution of the sodium salt in glyme was added 1 equiv of 2,2,2-cryptate in glyme. The resulting solution was stirred for several hours, after which a slow addition of hexane (or solvent diffusion of hexane into a glyme solution) produced a crystalline material.

Infrared spectra of the $[Na(2,2,2\text{-crypt})]^+$ salt in THF exhibited one bridging carbonyl band at 1670 (s) cm^{-1}, whereas two carbonyl bands at 1715 (w) and 1655 (s) cm^{-1} were observed in Nujol mull. EPR solution spectra were found to be invariant to either cation or solvent. A 0.01 M solution (THF) expectedly revealed a similar 15-line spectrum centered approximately at 3200 G with A_{iso} = 45 G and g_{iso} = 2.10. This spectrum is in accord with an analogous hyperfine interaction of the unpaired electron in the monoanion with both ^{59}Co nuclei.

Preparation and Physical Properties of the Neutral $Co_2(\eta^5\text{-}C_5Me_5)_2(\mu\text{-}CO)_2$ Dimer. (a) Method I. A C_5Me_5H sample (10 g, 40 mmol) was refluxed with $Co_2(CO)_8$ (12 g, 35 mmol) in CH_2Cl_2 (50 mL) for 16–18 h as described by Rausch and Genetti[22b] in their preparation of $Co(\eta^5\text{-}C_5H_5)(CO)_2$. The solution was then reduced in volume to 5 mL, after which it was chromatographed on an alumina column that was deoxygenated with degassed hexane. The $Co(\eta^5\text{-}C_5Me_5)(CO)_2$ product was eluted in hexane as a deep red band (14 g, 80% yield). The neutral $Co_2(\eta^5\text{-}C_5Me_5)_2(\mu\text{-}CO)_2$ dimer was eluted in a 4:1 hexane/toluene mixture. This emerald green compound (1.5 g, 10% yield) was identified by its characteristic IR, NMR, and mass spectral bands.

(b) Method II. To a sample of $[Na]^+[Co_2(\eta^5\text{-}C_5Me_5)_2(\mu\text{-}CO)_2]^-$ dissolved in THF was slowly added a stoichiometric quantity of a THF solution of anhydrous $FeCl_3$ over a 6–12-h period. The solvent was then removed under vacuum and the residue extracted with two 30-mL portions of toluene. The toluene extract was purified by chromatography on an alumina column. The neutral $Co_2(\eta^5\text{-}C_5Me_5)_2(\mu\text{-}CO)_2$ dimer was eluted with a 3:1 mixture of hexane/toluene.

(c) Method III. A solution of $Co(\eta^5\text{-}C_5Me_5)(CO)_2$ (2.0 g, 8.0 mmol) in tetrahydrofuran (175 mL) was photolyzed in a Pyrex glass apparatus continuously purged with nitrogen to facilitate the removal of evolved carbon monoxide. After 4 days an infrared spectrum of the reaction mixture indicated that all of the $Co(\eta^5\text{-}C_5Me_5)(CO)_2$

(19) Cirjak, L. M.; Ginsburg, R. E.; Dahl, L. F. *J. Chem. Soc., Chem. Commun.* **1979**, 470–472.
(20) Cirjak, L. M.; Huang, J.-S.; Zhu, Z.-H.; Dahl, L. F. *J. Am. Chem. Soc.* **1980**, *102*, 6623–6626.
(21) Threlkel, R. S.; Bercaw, J. E. *J. Organomet. Chem.* **1977**, *136*, 1–5.
(22) (a) King, R. B. "Organometallic Syntheses", Vol. I, Academic Press: New York, 1965; Vol. I, p 115–119. (b) Rausch, M. D.; Genetti, R. A. *J. Org. Chem.* **1970**, *35*, 3888–3897.
(23) (a) Ruff, J. K.; Schlientz, W. J. *Inorg. Synth.* **1974**, *15*, 84–87. (b) Pray, A. R. *Ibid.* **1975**, *5*, 153–165.

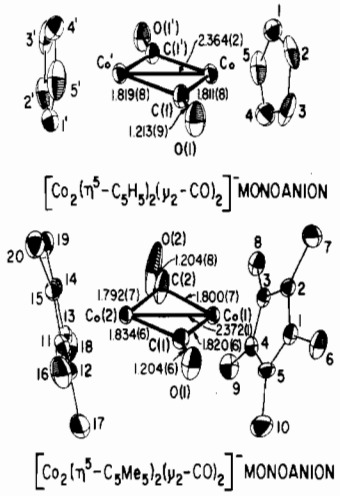

Figure 2. Configurations of the $[Co_2(\eta^5\text{-}C_5H_5)_2(\mu\text{-}CO)_2]^-$ and $[Co_2(\eta^5\text{-}C_5Me_5)_2(\mu\text{-}CO)_2]^-$ monoanions crystallized as the $[AsPh_4]^+$ and [Na(2,2,2-crypt)]$^+$ salts, respectively. The cyclopentadienyl carbon atoms are simply labeled by their respective number, *n*. The unsubstituted-cyclopentadienyl dimeric monoanion has a crystallographic center of inversion in contrast to no required symmetry for the pentamethyl-substituted cyclopentadienyl dimeric monoanion. A crystalline disorder of one of the two bridging carbonyl ligands in the nonplanar $Co_2(CO)_2$ core of the (pentamethylcyclopentadienyl)cobalt monoanion is readily apparent from the extensive out-of-plane elongation of the thermal ellipsoids of the C(2) and O(2) atoms relative to those of the other atoms in either monoanion.

had been consumed and only $Co_2(\eta^5\text{-}C_5Me_5)_2(\mu\text{-}CO)_2$ was present. The dark green solution was then transferred to another flask (leaving behind a small amount of insoluble blue residue) and the solvent removed under vacuum to yield a dark green crystalline solid (1.65 g, 93% yield). Photolyses carried out in a quartz reactor with toluene as the solvent were typically completed in 6–8 h with comparable high yields. However, a careful control of the photolysis time was necessary in order not to produce $Co_3(\eta^5\text{-}C_5Me_5)_2(CO)_3(\mu\text{-}CO)(\mu_3\text{-}CCH_3)$.[24]

IR spectra of the neutral dimer exhibited one strong carbonyl frequency at 1760 cm^{-1} in hexane, 1750 cm^{-1} in THF, and 1750 cm^{-1} in Nujol mull. A ^{1}H NMR spectrum in benzene-d_6 expectedly displayed a singlet at δ 1.40. A mass spectrum (IP = 70 eV, inlet temperature = 150 °C) gave a fragmentation pattern (which exhibited the parent ion peak) whose major ion peaks (*m/e*) and relative peak heights (in parentheses) are listed together with the assigned ion fragments as follows: *m/e* 444 (34.3), $(C_5(CH_3)_5)_2Co_2(CO)_2^+$; *m/e* 386 (100.0), $(C_5(CH_3)_4CH_2)_2Co_2^+$; *m/e* 329 (48.5), $(C_5(CH_3)_5)_2Co^+$; *m/e* 250 (14.1), $(C_5(CH_3)_5)Co(CO)_2^+$; *m/e* 222 (14.0), $(C_5(CH_3)_5)Co(CO)^+$; *m/e* 194 (8.9), $(C_5(CH_3)_5)Co^+$; *m/e* 192 (8.8), $(C_5(CH_3)_3)(CH_2)_2)Co^+$; *m/e* 134 (8.0), $(C_5(CH_3)_4CH_2)^+$; *m/e* 133 (8.0), $C_5(CH_3)_3(CH_2)_2^+$; *m/e* 119 (17.6), $C_9H_{11}^+$; *m/e* 91 (11.4), $C_7H_7^+$.

Structural Determinations of $[AsPh_4]^+[Co_2(\eta^5\text{-}C_5H_5)_2(\mu\text{-}CO)_2]^-$ (1a) and [Na(2,2,2-crypt)]$^+[Co_2(\eta^5\text{-}C_5Me_5)_2(\mu\text{-}CO)_2]^-$ (3a). Well-shaped single crystals of $[Ph_4As]^+[Co_2(\eta^5\text{-}C_5H_5)_2(\mu\text{-}CO)_2]^-$ and [Na(2,2,2-crypt)]$^+[Co_2(\eta^5\text{-}C_5Me_5)_2(\mu\text{-}CO)_2]^-$ were grown as described previously. The X-ray diffraction measurements were performed on a Syntex P$\bar{1}$ diffractometer with Mo K$\bar{\alpha}$ radiation. Details of the optical and X-ray alignment of each crystal as well as the method of data collection are analogous to those given elsewhere.[25]

The parallelepiped-shaped crystal of $[AsPh_4]^+[Co_2(\mu^5\text{-}C_5H_5)_2(\mu\text{-}CO)_2]^-$ selected for the collection of intensity data possessed the following crystal-face indices and perpendicular distances from its centroid: (111) and ($\bar{1}\bar{1}\bar{1}$), 0.18 mm; (20$\bar{1}$) and ($\bar{2}$01), 0.21 mm; ($\bar{1}$10) and (1$\bar{1}$0), 0.16 mm. The measured lattice constants for the determined monoclinic unit cell at 22 °C are a = 9.205 (5) Å, b = 19.888 (8) Å, c = 17.748 (9) Å, and β = 110.37 (4)°. The unit cell volume is 3046 (2) Å^3. The experimental density of 1.47 g/cm^3, measured by the flotation method, is in agreement with a calculated density of 1.50 g/cm^3 for Z = 4 and fw = 685. Observed systematic absences of $h + k = 2n + 1$ for {*hkl*} data and $l = 2n + 1$ for {*h*0*l*} data indicate the probable space group to be either $C2/c$ or Cc. The former centrosymmetric space group, whose choice was substantiated by the successful refinement of the crystal structure, requires that each $[AsPh_4]^+$ cation lie on a crystallographic twofold axis and that each monoanion lie on a crystallographic center of symmetry. The structural analysis thereby required the location of 1 arsenic atom, occupying a fourfold set of special equivalent positions at (0, 0, 0; $^1/_2$, $^1/_2$, 0) ± (0, y, $^1/_4$), and 1 cobalt, 1 oxygen, 18 carbon, and 15 hydrogen atoms, each occupying the eightfold set of general equivalent positions at (0, 0, 0; $^1/_2$, $^1/_2$, 0) ± (x, y, z; $\bar{x}$, y, $^1/_2 - z$). Intensity data for two independent reciprocal lattice octants were collected over a 2θ range of 3.0–45.0°; no correction for crystal decay was made in that a linear decrease of only 3% was measured for two standard reflections during the data collection. An analytical absorption correction[26a] was made in that the estimated transmission coefficients (based upon a calculated μ value of 23.0 cm^{-1} for Mo Kα radiation) varied from 0.32 to 0.62. A merging[26b] of the 2080 sampled data gave rise to 2004 independent reflections, of which the 1473 reflections with $I > 2\sigma(I)$ were used in the structural determination and refinement. The crystal structure was solved via the heavy-atom Patterson technique followed by Fourier syntheses,[26c] which located all nonhydrogen atoms. Hydrogen atoms were inserted at idealized positions, and the atomic parameters were then refined by block-diagonal[26d] and full-matrix[26e] least squares with anisotropic thermal parameters utilized for all nonhydrogen atoms and with hydrogen atoms included as fixed contributors with isotropic temperature factors. The final least-squares cycle converged to $R_1(F)$ = 5.3% and $R_2(F)$ = 6.0%[27] with the maximum value in the coordinate shift-to-error ratio in the final cycle being 0.06. The determined goodness-of-fit was 1.42 with the data-to-parameter ratio being 7.4:1. A final difference Fourier map, which showed the maximum residual peak to be only 1.3 e/Å^3, revealed no unusual features. Anomalous dispersion corrections[28] of the scattering factors[29] were made for arsenic and cobalt.

For [Na(2,2,2-crypt)]$^+[Co_2(\eta^5\text{-}C_5Me_5)_2(\mu\text{-}CO)_2]^-$, an orthorhombic-shaped crystal was chosen with the following crystal-face indices and perpendicular distances from its centroid: (100) and ($\bar{1}$00), 0.23 mm; (010) and (0$\bar{1}$0), 0.30 mm; (001) and (00$\bar{1}$), 0.32 mm. Diffraction data revealed the crystal to be monoclinic with lattice constants a = 17.364 (8) Å, b = 17.948 (4) Å, c = 13.903 (3) Å, β = 90.82 (3)°, and V = 4332 (2) Å^3. The flotation-measured density of 1.31 g/cm^3 is in accord with a calculated density of 1.29 g/cm^3 for Z = 4 and fw = 823. Observed systematic absences of $h = 2n + 1$ for {*h*0*l*} data and $k = 2n + 1$ for {0*k*0} data uniquely indicate the probable space

(24) Bailey, W. I., Jr.; Cotton, F. A.; Jamerson, J. D. *J. Organomet. Chem.* **1979**, *173*, 317–324.
(25) Byers, L. R.; Dahl, L. F. *Inorg. Chem.* **1980**, *19*, 277–284 and references therein.
(26) (a) Blount, J. F. "DEAR, a FORTRAN Absorption-Correction Program", 1965 (based on the method given by: Busing, W. R.; Levy, H. A. *Acta Crystallogr.* **1957**, *10*, 180–182). (b) Broach, R. W. "QUICKSAM, a FORTRAN Program for Sorting and Merging Structure Factor Data", Ph.D. Thesis, University of Wisconsin–Madison, 1977, Appendix II. (c) Calabrese, J. C. "MAP, a FORTRAN Summation and Molecular Assemblage Program", University of Wisconsin–Madison, 1972. (d) Calabrese, J. C. "A Crystallographic Variable Matrix Least-Squares Refinement Program", University of Wisconsin–Madison, 1972. (e) Busing, W. R.; Martin, K. O.; Levy, H. A. "OR FLS, a FORTRAN Crystallographic Least-Squares Program", Report ORNL-TM-305; Oak Ridge National Laboratory: Oak Ridge, Tenn., 1962. (f) Busing, W. R.; Martin, K. O.; Levy, H. A. "OR FEE, a FORTRAN Crystallographic Function and Error Program", Report ORNL-TM-306; Oak Ridge National Laboratory: Oak Ridge, Tenn., 1964. (g) Smith, D. L. "PLANES", Ph.D. Thesis, University of Wisconsin–Madison, 1962, Appendix IV. (h) Main, P.; Lessinger, L.; Woolfson, M. M.; Germain, G.; Declercq, J.-P. "MULTAN-76" (an updated version of MULTAN: Germain, G.; Main, P.; Woolfson, M. M. *Acta Crystallogr., Sect. A* **1971**, *A27*, 368–376). (i) Johnson, C. K. "OR TEP-II, A FORTRAN Thermal-Ellipsoid Plot Program for Crystal Structure Illustrations", Report ORNL-5138; Oak Ridge National Laboratory: Oak Ridge, Tenn., 1976.
(27) The unweighted and weighted discrepancy factors used are $R_1(F) = [\sum||F_o| - |F_c||/\sum|F_o|] \times 100$ and $R_2(F) = [\sum w_i||F_o| - |F_c||^2/\sum w_i|F_o|^2]^{1/2} \times 100$. All least-squares refinements were based on the minimization of $\sum w_i||F_o| - |F_c||^2$ with individual weights of $w_i = 1/\sigma^2(F_o)$.
(28) "International Tables for X-Ray Crystallography"; Kynoch Press: Birmingham, England, 1974; Vol. IV, p 149.
(29) Atomic scattering factors for neutral atoms were used (Cromer, D. T.; Mann, J. B. *Acta Crystallogr., Sect. A* **1968**, *A24*, 321–324. Stewart, R. F.; Davidson, E. R.; Simpson, W. T. *J. Chem. Phys.* **1965**, *42*, 3175–3187).

Table I. Atomic Parameters[a-c] for $[AsPh_4]^+[Co_2(\eta^5\text{-}C_5H_5)_2(\mu\text{-}CO)_2]^-$

A. Positional Parameters

	x	y	z		x	y	z
Co	0.42787 (12)	0.03432 (5)	0.44542 (6)	CB(4)	0.9217 (12)	0.0708 (5)	0.8906 (5)
O(1)	0.6832 (8)	0.0998 (3)	0.5619 (4)	CB(5)	0.7779 (12)	0.0548 (4)	0.8927 (5)
C(1)	0.5984 (10)	0.0528 (5)	0.5328 (5)	CB(6)	0.6532 (10)	0.0938 (4)	0.8498 (5)
CP(1)	0.2092 (11)	0.0685 (8)	0.3741 (8)	H(1)	0.1043	0.0555	0.3829
CP(2)	0.2806 (26)	0.0364 (5)	0.3256 (7)	H(2)	0.2344	−0.0082	0.2881
CP(3)	0.4116 (19)	0.0729 (10)	0.3341 (8)	H(3)	0.4862	0.0544	0.3011
CP(4)	0.4178 (14)	0.1233 (8)	0.3826 (9)	H(4)	0.5156	0.1543	0.3900
CP(5)	0.2981 (19)	0.1222 (6)	0.4077 (6)	H(5)	0.2944	0.1614	0.4465
As	1/2 (−)	0.20359 (5)	3/4 (−)	HA(2)	0.4564	0.1902	0.5792
CA(1)	0.5501 (8)	0.2581 (4)	0.6748 (4)	HA(3)	0.5323	0.2610	0.4840
CA(2)	0.5146 (13)	0.2368 (5)	0.5974 (5)	HA(4)	0.6825	0.3635	0.5318
CA(3)	0.5594 (17)	0.2761 (6)	0.5445 (6)	HA(5)	0.7369	0.4016	0.6675
CA(4)	0.6412 (12)	0.3342 (5)	0.5694 (5)	HA(6)	0.6542	0.3339	0.7606
CA(5)	0.6740 (10)	0.3551 (4)	0.6459 (5)	HB(2)	0.8328	0.2063	0.7685
CA(6)	0.6292 (10)	0.3176 (4)	0.6994 (5)	HB(3)	1.0537	0.1328	0.8407
CB(1)	0.6722 (9)	0.1478 (4)	0.8052 (4)	HB(4)	1.0202	0.0416	0.9242
CB(2)	0.8178 (10)	0.1634 (5)	0.8029 (5)	HB(5)	0.7647	0.0132	0.9261
CB(3)	0.9417 (10)	0.1227 (6)	0.8461 (6)	HB(6)	0.5389	0.0819	0.8495

B. Anisotropic Thermal Parameters ($\times 10^5$)[b]

	β_{11}	β_{22}	β_{33}	β_{12}	β_{13}	β_{23}		β_{11}	β_{22}	β_{33}	β_{12}	β_{13}	β_{23}
Co	911	316	319	93	121	71	CA(3)	5050	526	333	−577	739	−120
O(1)	1873	397	638	−182	−193	96	CA(4)	2311	441	431	−218	413	94
C(1)	1096	388	350	88	−13	30	CA(5)	1650	337	414	−259	234	−4
Cp(1)	724	581	796	127	127	357	CA(6)	1270	374	310	−147	127	−2
Cp(2)	4596	297	414	198	−734	13	CB(1)	921	297	316	55	109	−18
Cp(3)	3120	824	384	753	588	256	CB(2)	1224	412	479	134	187	105
Cp(4)	1340	677	732	−174	−23	389	CB(3)	1062	568	578	96	263	74
Cp(5)	3251	354	416	535	158	75	CB(4)	1670	404	441	397	172	43
As	895	254	281	0	130	0	CB(5)	1838	296	445	280	246	109
CA(1)	924	271	304	20	119	−0	CB(6)	1438	286	400	12	332	9
CA(2)	3536	380	370	−480	563	−126							

C. Root-Mean-Square Thermal Displacements (Å) of Selected Atoms along Their Principal Ellipsoidal Axes

	μ(1)	μ(2)	μ(3)		μ(1)	μ(2)	μ(3)		μ(1)	μ(2)	μ(3)
Co	0.17	0.22	0.26	C(1)	0.18	0.27	0.28	O(1)	0.22	0.26	0.39

[a] The estimated standard deviations of the least significant figures are given in parentheses. [b] Anisotropic temperature factors are of the form $\exp\{-[\beta_{11}h^2 + \beta_{22}k^2 + \beta_{33}l^2 + 2\beta_{12}hk + 2\beta_{13}hl + 2\beta_{23}kl]\}$. [c] In the final full-matrix least-squares cycle performed on a HARRIS/7 computer only the positional parameters of the nonhydrogen atoms were varied. All anisotropic and isotropic thermal parameters as well as the positional parameters of the hydrogen atoms were assigned as fixed contributors obtained from a previous converged block-diagonal refinement. Idealized hydrogen positions (at distances of 0.90 Å from their attached carbon atoms) were not varied during least-squares refinement but were recalculated after every other cycle so as to take into account the shifts in positions of the carbon atoms. The arbitrarily assigned thermal parameters of 6.0 Å² for all hydrogen atoms were held constant.

group to be $P2_1/a$. This centrosymmetric space group, whose selection is completely compatible with the refinement of the crystal structure, results in the crystallographically independent unit being composed of one monocation and one monoanion with C_1-1 site symmetry. Hence, the structural determination necessitated the location of 1 sodium, 2 cobalt, 8 oxygen, 2 nitrogen, 40 carbon, and 66 hydrogen atoms, each occupying the fourfold set of general equivalent positions at $\pm(x, y, z; {}^1/_2 - x, {}^1/_2 + y, \bar{z})$. Two independent, intensity-weighted reciprocal lattice octants were sampled over a 2θ range of 3.0–45.0°; an intensity correction for crystal decay was necessary in that a linear decrease of 25% was determined for the intensities of the two standard reflections during the data collection. Since the estimated transmission coefficients (based upon a calculated μ value of 8.36 cm^{-1} for Mo Kα radiation) ranged from 0.60 to 0.71, an analytical absorption correction[26a] was also applied to the intensity data. A merging[26b] of the 6138 intensity-measured reflections gave 5686 independent ones, of which the 4033 reflections with $I > 2\sigma(I)$ were utilized in the structural analysis and refinement. The crystal structure was solved and all nonhydrogens were located from Patterson-Fourier syntheses.[26c] Idealized coordinates were estimated for each hydrogen atom from the assumed regular geometry of each attached carbon atom. Least-squares refinement[26e] with anisotropic thermal parameters for all nonhydrogen atoms and fixed isotropic temperature factors for the nonvarying hydrogen atoms converged at $R_1(F) = 6.0\%$ and $R_2(F) = 6.9\%$[27] with no coordinate shift-to-error ratio in the final cycle being greater than 0.25. The goodness-of-fit values was 1.50, while the data-to-parameter ratio was 8.4:1. A final difference Fourier map showed no maximum residual peak greater than 0.8 e/Å³. Anomalous dispersion corrections[28] were applied to the scattering factors[29] of cobalt and sodium.

For $[AsPh_4]^+[Co_2(\eta^5\text{-}C_5H_5)_2(\mu\text{-}CO)_2]^-$ the final atomic positional and thermal parameters are given in Table I, bond lengths and angles with esds[26f] are presented in Table II, and selected least-squares planes and interplanar angles[26g] are given in Table III. The analogous information for $[Na(2,2,2\text{-crypt})]^+[Co_2(\eta^5\text{-}C_5Me_5)_2(\mu\text{-}CO)_2]^-$ is included in Tables IV, V, and VI, respectively. The observed and calculated structure factors as well as Tables III and VI are given as supplementary material.

Structural Determination of $Co_2(\eta^5\text{-}C_5Me_5)_2(\mu\text{-}CO)_2$ (4). Crystals suitable for X-ray diffraction were grown by slow evaporation of a hexane solution (via vapor diffusion into decalin) of $Co_2(\eta^5\text{-}C_5Me_5)_2(\mu\text{-}CO)_2$. A dark green orthorhombic-shaped crystal of dimensions 0.58 × 0.42 × 0.40 mm was mounted inside a thin-walled Lindemann glass capillary, which was evacuated, filled with argon, and then flame-sealed. Diffraction data, which conformed to monoclinic Laue symmetry C_{2h}-$2/m$, provided lattice constants (at 23 °C) of $a = 9.693$ (5) Å, $b = 14.722$ (7) Å, $c = 14.912$ (6) Å, $\beta = 101.86$ (4)° and $V = 2083$ (2) Å.³ The calculated density of 1.42 g/cm³ corresponds to $Z = 4$ and fw = 444. Observed systematic absences of $l = 2n + 1$ for $\{h0l\}$ and $k = 2n + 1$ for $\{0k0\}$ uniquely define the probable space group to be $P2_1/c$. This centrosymmetric space group gives rise to the crystallographically independent unit consisting of one dimeric molecule with no special site symmetry. Therefore, the structural determination required the location of 2 cobalt, 2 oxygen, 22 carbon, and 30 hydrogen atoms, each occupying the fourfold set of general equivalent positions $\pm(x, y, z; \bar{x}, {}^1/_2 + y,$

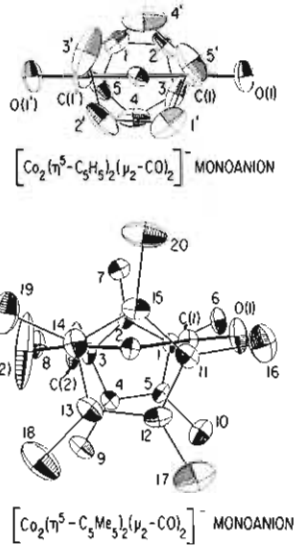

Figure 3. Configurations of the $[Co_2(\eta^5\text{-}C_5H_5)_2(\mu\text{-}CO)_2]^-$ and $[Co_2(\eta^5\text{-}C_5Me_5)_2(\mu\text{-}CO)_2]^-$ monoanions viewed along their Co–Co′ directions, emphasizing the perpendicular and distinctly nonperpendicular dispositions of the C_5H_5 and C_5Me_5 rings, respectively, relative to their $Co_2(CO)_2$ cores. The nature and extent of the considerable distortion of the $Co_2(CO)_2$ core in the $[Co_2(\eta^5\text{-}C_5Me_5)_2(\mu\text{-}CO)_2]^-$ monoanion from planarity are also evident, with the usually elongated thermal ellipsoids of C(2) and O(2) being readily interpreted in terms of a disorder-averaged structure involving the superposition of at least two bent orientations of the bridging C(2)–O(2) ligand.

$^1/_2 - z$). The intensities of 2980 reflections from two independent reciprocal lattice octants were measured between the 2θ limits of 3.0–45.0°. No significant changes in the intensities of the two standard reflections were observed during data collection. Examination of several ψ scans indicated no need for an absorption correction. A data merging[26b] gave 2780 independent reflections, of which the 1720 maxima with $I > 2\sigma(I)$ were utilized in the structural analysis and refinement. The structure was solved via direct methods[26h] followed by Fourier and difference Fourier syntheses,[26c] which yielded the positions of all nonhydrogen atoms as well as those of a number of methyl hydrogen atoms. Idealized coordinates for all the hydrogen atoms were then calculated, and the structure was refined by combined block-diagonal[26d] and full-matrix[26e] least squares. The thermal parameters for all nonhydrogen atoms were refined anisotropically, while the hydrogen atoms were included with fixed positions and fixed isotropic temperature factors. The final cycle of the full-matrix, least-squares refinement converged to $R_1(F) = 7.2\%$ and $R_2(F) = 7.8\%$[27] with no parameter shift-to-error ratio being greater than 0.01. The standard error-of-fit was 1.70, while the data-to-parameter ratio was 7.3:1. A final Fourier difference map exhibited no unusual features. Anomalous dispersion corrections[28] were applied to the scattering factors[29] of cobalt.

The atomic parameters from the output of the last cycle are presented in Table VII. Interatomic distances and bond angles[26f] are listed in Table VIII, while selected least-squares planes and interplanar angles[26g] are given in Table IX. The observed and calculated structure factors together with Table IX are given as supplementary material.

Results and Discussion

Structural Description and Comparison between Monoanions of $[AsPh_4]^+[Co_2(\eta^5\text{-}C_5H_5)_2(\mu\text{-}CO)_2]^-$ and $[Na(2,2,2\text{-crypt})]^+[Co_2(\eta^5\text{-}C_5Me_5)_2(\mu\text{-}CO)_2]^-$. (a) Structural Features of $[AsPh_4]^+[Co_2(\eta^5\text{-}C_5H_5)_2(\mu\text{-}CO)_2]^-$. Its crystal structure consists of dimeric monoanions (Figures 2 and 3) with site symmetry $C_i\text{-}\bar{1}$ and tetraphenylarsonium cations with site symmetry C_2-2. The cations and monoanions are well separated from one another, as indicated in a unit cell diagram (Figure 4), with no interionic distances being less than 3.4 Å. The configuration of the $[AsPh_4]^+$ cation expectedly exhibits no unusual features and is not unlike those found in the crystal structures of other tetraphenylarsonium salts.

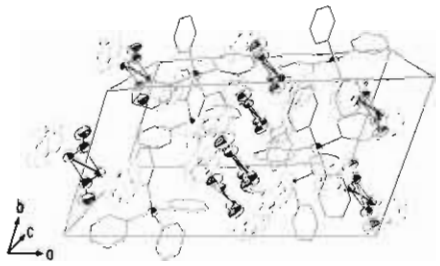

Figure 4. View of the monoclinic unit cell of $[AsPh_4]^+[Co_2(\eta^5\text{-}C_5H_5)_2(\mu\text{-}CO)_2]^-$ showing the arrangement under $C2/c$ symmetry of the four cations of crystallographic C_2-2 site symmetry and the four dimeric monoanions of crystallographic $C_i\text{-}\bar{1}$ site symmetry.

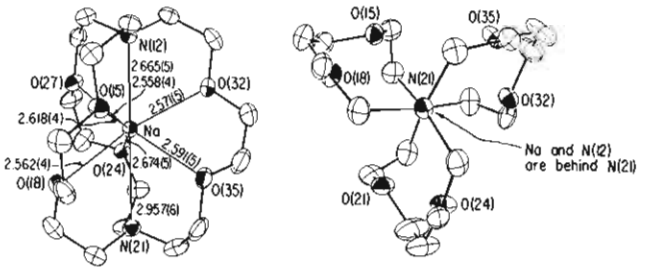

Figure 5. Two views of the $[Na(2,2,2\text{-crypt})]^+$ cation (where 2,2,2-crypt denotes $N(C_2H_4OC_2H_4OC_2H_4)_3N$) of the $[Co_2(\eta^5\text{-}C_5Me_5)_2(\mu\text{-}CO)_2]^-$ salt showing (on the right side) the pseudo-C_3-3 principal axis of the cryptate ligand viewed down the N(21)–Na–N(12) axis and (on the left side) the highly asymmetrical coordination of the encapsulated Na^+ ion, with one long Na^+–N distance of 2.957 (6) Å vs. the other Na^+–N distance of 2.665 (5) Å and the six Na^+–O distances of range 2.558 (4)–2.674 (5) Å. this particular variation of the eight Na^+ contacts with two nitrogen and six oxygen atoms of the heteroatom polyhedron may be readily attributed to the Na^+ residing in too large a cryptate cavity.

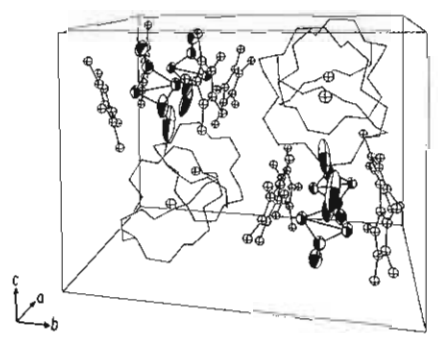

Figure 6. View of the monoclinic unit cell of $[Na(2,2,2\text{-crypt})]^+[Co_2(\eta^5\text{-}C_5Me_5)_2(\mu\text{-}CO)_2]^-$ showing the arrangement of the four cations and four monoanions under $P2_1/c$ symmetry.

The solid-state geometry of the $[Co_2(\eta^5\text{-}C_5H_5)_2(\mu\text{-}CO)_2]^-$ monoanion shows a strictly planar $Co_2(CO)_2$ core, as required by the center of inversion. The independent cyclopentadienyl ring, whose ring carbon atoms are coplanar within 0.005 Å, is perpendicular within 0.6° to the planar $Co_2(CO)_2$ core. The Co–Co distance of 2.364 (2) Å and the mean Co–CO distance of 1.815 Å are in close agreement with corresponding values of 2.366 Å (the mean of 2.359 (2) and 2.372 (2) Å) and 1.82 Å reported by Schore, Ilenda, and Bergman[2] for the two crystallographically independent half-dimers of this monoanion in the $[PPN]^+$ salt and with the values of 2.370 (1) and 1.829 (7) Å reported by Bernal et al.[11] for the isoelectronic $Co_2(\eta^5\text{-}C_5H_5)_2(\mu\text{-}CO)(\mu\text{-}NO)$ molecule, for which the bridging nitrosyl and carbonyl bridging ligands are centrosymmetrically disordered in the crystalline state (see Table X).

(b) Structural Features of $[Na(2,2,2\text{-crypt})]^+[Co_2(\mu^5\text{-}C_5Me_5)_2(\mu\text{-}CO)_2]^-$. Its crystal structure is composed of one independent cation (Figure 5) and one independent monoanion

Table II. Interatomic Distances and Bond Angles for $[AsPh_4]^+[Co_2(\eta^5\text{-}C_5H_5)_2(\mu\text{-}CO)_2]^-$

A. Intraanion Distances (Å) Averaged under Assumed D_{2h} Symmetry

Co-Co′	2.364 (2)[a]	Co-Cp(1)	2.083 (9)
C(1)···(C1′)	2.75 (2)	Co-Cp(2)	2.087 (10)
		Co-Cp(3)	2.076 (10)
Co-C(1)	1.819 (8)	Co-Cp(4)	2.077 (11)
Co-C(1′)	1.811 (10)	Co-Cp(5)	2.090 (9)
	1.815 (av)		2.083 (av)
Co···O(1)	2.849 (7)	Cp(1)-Cp(2)	1.40 (2)
Co···O(1′)	2.845 (7)	Cp(2)-Cp(3)	1.37 (2)
	2.847 (av)	Cp(3)-Cp(4)	1.31 (2)
C(1)-O(1)	1.213 (10)	Cp(4)-Cp(5)	1.32 (2)
Co-Cp(c)[b]	1.737	Cp(5)-Cp(1)	1.35 (2)
			1.35 (av)

B. Intraanion Angles (Deg) Averaged under Assumed D_{2h} Symmetry

Co-C(1)-Co′	81.3 (4)	Cp(c)-Co-Co′	179.4
C(1)-Co-C(1′)	98.7 (4)	Cp(c)-Co-C(1)	130.6
Co-C(1)-O(1)	139.2 (7)	Cp(c)-Co-C(1′)	130.7
Co′-C(1)-O(1)	139.5 (7)		130.6 (av)
	139.4 (av)	Cp(1)-Cp(2)-Cp(3)	106 (1)
		Cp(2)-Cp(3)-Cp(4)	108 (1)
		Cp(3)-Cp(4)-Cp(5)	111 (1)
		Cp(4)-Cp(5)-Cp(1)	108 (1)
		Cp(5)-Cp(1)-Cp(2)	107 (1)
			108 (av)

C. Intracation Distances (Å)

As-CA(1)	1.897 (7)	CB(1)-CB(2)	1.391 (11)
As-CB(1)	1.903 (8)	CB(2)-CB(3)	1.391 (12)
	1.900 (av)	CB(3)-CB(4)	1.351 (12)
CA(1)···CB(1)	3.102 (10)	CB(4)-CB(5)	1.374 (13)
CA(1)···CB(1″)	3.114 (11)	CB(5)-CB(6)	1.375 (11)
	3.108 (av)	CB(6)-CB(1)	1.380 (10)
			1.377 (av)
CA(1)-CA(2)	1.363 (10)		
CA(2)-CA(3)	1.390 (12)		
CA(3)-CA(4)	1.366 (13)		
CA(4)-CA(5)	1.349 (12)		
CA(5)-CA(6)	1.379 (11)		
CA(6)-CA(1)	1.379 (11)		
	1.371 (av)		

D. Intracation Angles (Deg)

CA(1)-As-CB(1)	109.4 (3)	As-CB(1)-CB(2)	119.5 (6)
CA(1)-As-CB(1″)	104.6 (2)	As-CB(1)-CB(6)	120.0 (6)
	107.0 (av)		119.8 (av)
As-CA(1)-CA(2)	120.0 (6)	CB(1)-CB(2)-CB(3)	117.8 (8)
As-CA(1)-CA(6)	119.9 (6)	CB(2)-CB(3)-CB(4)	121.0 (8)
	120.0 (av)	CB(3)-CB(4)-CB(5)	121.4 (8)
		CB(4)-CB(5)-CB(6)	118.7 (8)
CA(1)-CA(2)-CA(3)	118.8 (8)	CB(5)-CB(6)-CB(1)	120.5 (8)
CA(2)-CA(3)-CA(4)	121.2 (8)	CB(6)-CB(1)-CB(2)	120.4 (7)
CA(3)-CA(4)-CA(5)	119.4 (8)		
CA(4)-CA(5)-CA(6)	120.8 (8)		
CA(5)-CA(6)-CA(1)	119.8 (7)		
CA(6)-CA(1)-CA(2)	120.0 (7)		
	120.0 (av)		

E. Intraionic and Interionic Nonbonding Distances (Å)

CA(2)···O(1)	3.30 (1)	Cp(4)···O(1)	3.30 (1)
HA(2)···O(1)	2.85 (1)	Cp(1)···O(1′)	3.56 (1)
		Cp(2)···O(1′)	3.30 (1)

[a] Atoms with single primes (e.g., Co′) refer to the symmetry-related positional $1-x, -y, 1-z$; atoms with double primes (e.g., CB(1″)) refer to the symmetry-related position $1-x, y, \frac{1}{2}-z$. [b] Cp(c) refers to the centroid of the five cyclopentadienyl carbon atoms (viz., Cp(1), Cp(2), Cp(3), Cp(4), and Cp(5)).

(Figures 2 and 3). The arrangement of the four cations and the four monoanions in the monoclinic unit cell is shown in Figure 6. There is no evidence for unusual interionic interactions in the unit cell in that all nonhydrogen interionic distances are greater than 3.4 Å. The $[Na(2,2,2\text{-crypt})]^+$ cation (Figure 5) is composed of a macrobicyclic diamino hexaether, which completely encapsulates the sodium ion. Its overall geometry (including the particular asymmetrical coordination) is similar to that determined from an X-ray diffraction study[30] of $[Na(2,2,2\text{-crypt})]_2^+[Fe_2(CO)_6(\mu\text{-}PPh_2)_2]^{2-}$.

(c) Structural Comparison of the $[Co_2(\eta^5\text{-}C_5R_5)_2(\mu\text{-}CO)_2]^-$ Monoanions (Where R = H, Me). The solid-state geometry of the $[Co_2(\eta^5\text{-}C_5Me_5)_2(\mu\text{-}CO)_2]^-$ monoanion is significantly different from those found for the $[Co_2(\eta^5\text{-}C_5H_5)_2(\mu\text{-}CO)_2]^-$ monoanion and the $Co_2(\eta^5\text{-}C_5H_5)_2(\mu\text{-}CO)(\mu\text{-}NO)$ molecule. First, the $Co_2(CO)_2$ core is significantly nonplanar as shown by torsional angles of 168.0° between the two fused CoC_2 planes and of 169.6° between the two fused CCo_2 planes. Second, the C_5Me_5 ligands are not parallel to each other but are inclined with an angle of 153.5° between the ring normals. Figure 3 reveals that the two C_5Me_5 rings are also oriented in an almost eclipsed conformation in contrast to the staggered conformation found for the two C_5H_5 rings in the $[Co_2(\eta^5\text{-}C_5H_5)_2(\mu\text{-}CO)_2]^-$ monoanion and the other centrosymmetric dimers (Table X). Third, one of the two bridging carboxyl ligands in the dimeric (pentamethylcyclopentadienyl)cobalt monoanion displays extremely large out-of-plane thermal ellipsoids (Figures 2, 3, and 6) indicative of an averaged structure in which the one bridging carbonyl occupies at least two bent orientations in the crystalline state.

Figure 3 indicates that this large carbonyl displacement from a normal equilibrium position may be readily ascribed to intraanionic steric overcrowding primarily involving repulsions between this carbonyl ligand and one of the methyl substituents in each of the C_5Me_5 rings. However, an examination of intraanionic distances for both carbonyl ligands in the $[Co_2(\eta^5\text{-}C_5Me_5)_2(\mu\text{-}CO)_2]^-$ monoanion provides no clear-cut evidence of steric effects being responsible for this presumed crystal disorder of only *one* of the *two* bridging carbonyl ligands among two or more orientations. The existence of such an asymmetric, disordered solid-state structure involving only *one* instead of both bridging carbonyl ligands (even in a sterically crowded dimer) is certainly surprising.

Strong evidence that this nonplanar distortion of the $Co_2(CO)_2$ core in the $[Co_2(\eta^5\text{-}C_5Me_5)_2(\mu\text{-}CO)_2]^-$ monoanion as the $[Na(2,2,2\text{-crypt})]^+$ salt is limited to the solid state is indicated from its Nujol mull IR spectrum vs. solution IR spectra in the carbonyl stretching region. Whereas an IR spectrum

(30) Ginsburg, R. E.; Rothrock, R. K.; Finke, R. G.; Collman, J. P.; Dahl, L. F. *J. Am. Chem. Soc.* **1979**, *101*, 6550–6562.

(31) A quantitative indication of this unusually large out-of-plane thermal displacement of the C(2) and O(2) atoms in this one bridging carbonyl ligand relative to those of the carbon and oxygen atoms in the other bridging carbonyl ligand of the $[Co_2(\eta^5\text{-}C_5Me_5)_2(\mu\text{-}CO)_2]^-$ monoanion and in the one independent bridging carbonyl ligand of the centrosymmetric $[Co_2(\eta^5\text{-}C_5H_5)_2(\mu\text{-}CO)_2]^-$ monoanion can be obtained from an analysis of the atomic thermal ellipsoids, for each of which the root-mean-square components of thermal displacement (i.e., $\mu(r)$) have been calculated.[26f] The thermal ellipsoids of the cobalt atoms in both structures as well as of C(1) and O(1) in the cyclopentadienyl cobalt monoanion and C(1) and O(1) in the (permethylcyclopentadienyl)cobalt monoanion are symmetrically positioned with respect to the $Co_2(CO)_2$ plane with the largest principal axis component, $\mu(3)$, essentially perpendicular to that plane. An isotropic root-mean-square value of 0.20 Å for the cobalt atoms within the $Co_2(CO)_2$ plane (i.e., taken as the mean of $\mu(1)$ and $\mu(2)$ for the three independent atoms in both structures) is only 0.02 Å less than that of 0.22 Å for all of the carbonyl carbon and oxygen atoms in the $Co_2(CO)_2$ plane (i.e., taken as the mean of $\mu(1)$ and $\mu(2)$ for all of the carbon and oxygen atoms in both structures). These symmetric values can be compared to values for $\mu(3)$, which is the component approximately perpendicular to the $Co_2(CO)_2$ plane. For the $[Co_2(\eta^5\text{-}C_5H_5)_2(\mu\text{-}CO)_2]^-$ monoanion there is a small increase in $\mu(3)$ to 0.26 and 0.28 Å for Co and C(1), respectively; the value of 0.39 Å for O(1) is reasonably larger, as would be expected for a carbonyl oxygen atom. These magnitudes also compare quite closely to those calculated for Co(1), Co(2), C(1), and O(1) in the $[Co_2(\eta^5\text{-}C_5Me_5)_2(\mu\text{-}CO)_2]^-$ monoanion, thereby indicating no unusual thermal motion for the C(1)–O(1) ligand. However, the calculated values of $\mu(3)$ for C(2) and O(2) are 0.57 and 0.92 Å, respectively.

in Nujol mull exhibits two carbonyl frequencies at 1715 (w) and 1650 (s) cm^{-1} with the intensity pattern being characteristic of the symmetric and antisymmetric C–O stretching modes, respectively, only one carbonyl frequency at 1670 (s) cm^{-1} is observed in an IR spectrum of this monoanion in THF solution. The corresponding IR spectra for the planar $Co_2(CO)_2$ core of the $[Co_2(\eta^5\text{-}C_5H_5)_2(\mu\text{-}CO)_2]^-$ monoanion expectedly display a single carbonyl band at 1680 cm^{-1} as a Nujol mull and at 1690 cm^{-1} in THF solution.

The above geometrical change on going from solution to the crystalline state is the reverse of that observed in the two $Ni_2(\eta^5\text{-}C_5H_4R)_2(\mu\text{-}CO)_2$ dimers (R = H, Me),[15] for which KBr pellet and solution IR spectra in the bridging carbonyl region indicate in accordance with their determined crystallographic structures that the $Ni_2(CO)_2$ cores of both dimers are analogously bent in solution in contrast to the solid state where the $Ni_2(CO)_2$ core is planar in the methylcyclopentadienyl dimer but bent in the unsubstituted cyclopentadienyl dimer. It is noteworthy that a low-energy, dynamic butterfly-like interconversion involving both carbonyl ligands has been proposed[15] to occur in solution for the bent $Ni_2(CO)_2$ core of the sterically innocent $Ni_2(\eta^5\text{-}C_5H_5)_2(\mu\text{-}CO)_2$ molecule.

The amount of energy involved in a nonplanar deformation of a planar $Co_2(CO)_2$ core no doubt is small. Studies[32] on the influence of crystal packing upon molecular conformations estimate the lattice energy stabilization to be as low as several kilocalories per mole. Since it follows from electronic considerations (vide infra) that an isolated $M_2(\eta^5\text{-}C_5R_5)_2(\mu\text{-}CO)_2$-type dimer containing a metal–metal BO greater than 1.0 (e.g., these dimeric cobalt monoanions correspond to a Co–Co BO of 1.5) would prefer to be planar, it is presumed that the observed solid-state distortion of the $Co_2(CO)_2$ core in the $[Co_2(\eta^5\text{-}C_5Me_5)_2(\mu\text{-}CO)_2]^-$ monoanion must be induced by unsymmetrical packing interactions superimposed on the significant intraanionic steric effects due to repulsions between the pentamethylcyclopentadienyl and carbonyl ligands.

Since both Co–CO bond lengths involving this carbonyl ligand C(2)–O(2) with the larger thermal ellipsoids are expectedly shorter (viz., by 0.031 Å (average)) than those involving the well-behaved carbonyl ligand C(1)–O(1), only the distances and bond angles of this latter ligand are deemed to be reliable and hence are utilized in our comparisons (Table X) with other dimers.

The Co–Co distance and mean Co–CO distance of 2.372 (1) Å and 1.827 Å, respectively, in the $[Co_2(\eta^5\text{-}C_5Me_5)_2(\mu\text{-}CO)_2]^-$ monoanion of the $[Na(2,2,2\text{-crypt})]^+$ salt compare favorably (within 0.01 Å) with those found in the $[Co_2(\eta^5\text{-}C_5H_5)_2(\mu\text{-}CO)_2]^-$ monoanion of the $[AsPh_4]^+$ and $[PPN]^+$ salts (see Table X). Hence, there is no significant bond length evidence of increased $d_\pi(Co)\rightarrow\pi^*(CO)$ back-bonding when pentamethylcyclopentadienyl ligands are substituted in place of unsubstituted ones. This insensitivity is consistent with an observed difference in the carbonyl IR stretching frequency of only 20 cm^{-1} between the two monoanions in THF solution.

Structural Description of $Co_2(\eta^5\text{-}C_5Me_5)_2(\mu\text{-}CO)_2$ and Comparison to the $[Co_2(\eta^5\text{-}C_5Me_5)_2(\mu\text{-}CO)_2]^-$ Monoanion. The crystal structure of $Co_2(\eta^5\text{-}C_5Me_5)_2(\mu\text{-}CO)_2$ is composed of discrete molecules with an idealized configuration of C_{2v}-$m2m$ symmetry (Figure 7). The overall solid-state geometry of this molecule consists of a pair of cobalt atoms joined together by two symmetrically bridging carbonyl ligands to form a nearly planar $Co_2(CO)_2$ core with a C_5Me_5 ligand attached to each cobalt in an η^5 linkage.

There are distinct geometrical differences between the solid-state structures of the $Co_2(\eta^5\text{-}C_5Me_5)_2(\mu\text{-}CO)_2$ neutral dimer and both $[Co_2(\eta^5\text{-}C_5R_5)_2(\mu\text{-}CO)_2]^-$ (R = H, Me) monoanions. The $Co_2(CO)_2$ core of the neutral dimer (Figure 7) corresponds very closely to an ideal C_{2v}-$m2m$ geometry with the two C_5Me_5 ligands being in an eclipsed formation and bisected by one of the two pseudovertical mirror planes, which are perpendicular to the mean $Co_2(CO)_2$ plane. The C_5Me_5 ligands are nearly parallel, with the angle between the normals of the two rings being 178.1°. The $Co_2(CO)_2$ core deviates only slightly from planarity with CCo_2–Co_2C and CoC_2–C_2Co torsional angles of 176.3 and 175.4°, respectively. The existence of two eclipsed (rather than the normally staggered) C_5Me_5 rings as well as the other distortions from C_{2v} symmetry (Figure 7) may be attributed to a minimization of steric interactions between the C_5Me_5 ligands and the bridging carbonyls.

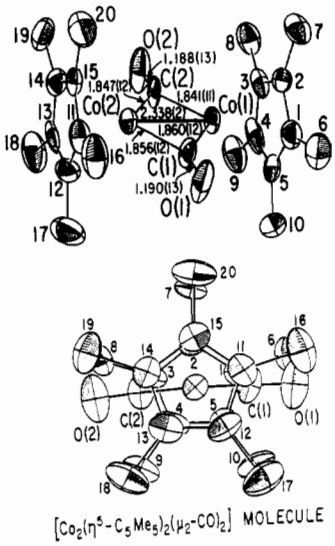

Figure 7. Two views of the neutral $Co_2(\eta^5\text{-}C_5Me_5)_2(\mu\text{-}CO)_2$ molecule of crystallographic C_1-1 site symmetry. The eclipsed conformation of the two C_5Me_5 rings, which are essentially perpendicular to the nearly planar $Co_2(CO)_2$ core, gives rise to an idealized C_{2v}-$m2m$ molecular geometry with the pseudotwofold axis perpendicular to the mean $Co_2(CO)_2$ plane. The observed slight puckering (bottom view) of the $Co_2(CO)_2$ core by only 4–5° from planarity may be attributed to steric effects involving the C_5Me_5 rings in that the electronic structure of this metal–metal double-bonded $Co_2(CO)_2$ core energetically favors its possessing a planar geometry.

A closer examination of the $Co_2(CO)_2$ core reveals other significant changes that occur upon oxidation of the monoanion to the neutral dimer. In the dimeric monoanion, the Co–Co and Co–CO bond distances are 2.372 (1) and 1.827 (average) Å, respectively, while the corresponding distances in its oxidized neutral dimer are 2.338 (2) and 1.851 (average) Å, respectively. Hence, removal of an electron from the monoanion results in a *shortening* of the Co–Co bond distance by 0.034 Å, together with a coincident *lengthening* of the average Co–CO bond distance by 0.024 Å. These opposite bond length changes necessarily require a 4.0° angular increase in the mean OC–Co–CO bond angles from 97.6° in the monoanion to 101.6° in the neutral dimer; there is a corresponding 2.6° angular decrease in the mean Co–C(O)–Co bond angle from 81.0° in the monoanion to 78.4° in the neutral dimer. The mean Co–Cp(centroid) distances are 1.736 and 1.697 Å for the monoanion and neutral dimer, respectively.

The presence in the solid-state spectra of one bridging carbonyl band (at 1750 cm^{-1}) for the neutral dimer and two bands (at 1715 (w) and 1655 (s) cm^{-1}) for its monanion is in accordance with their determined structures in the crystalline state. The higher and lower frequencies may be readily assigned to symmetric and asymmetric C–O stretching modes, respectively, in $[Na(2,2,2\text{-crypt})]^+[Co_2(\eta^5\text{-}C_5Me_5)_2(\mu\text{-}CO)_2]^-$, while in $Co_2(\eta^5\text{-}C_5Me_5)_2(\mu\text{-}CO)_2$ the single frequency is at-

(32) Brock, C. P. *Acta Crystallogr., Sect. A* **1977**, *A33*, 193–197. Bernstein, J.; Hagler, A. T. *J. Am. Chem. Soc.* **1978**, *100*, 673–681.

Table IV. Atomic Parameters[a-d] for $[Na(2,2,2\text{-crypt})]^+[Co_2(\eta^5\text{-}C_5Me_5)_2(\mu\text{-}CO)_2]^-$

A. Positional Parameters

	x	y	z		x	y	z
Co(1)	0.22638 (5)	0.17750 (4)	0.25745 (5)	HCp(8B)	0.3319	0.1243	0.4583
Co(2)	0.22453 (5)	0.30686 (4)	0.22255 (5)	HCp(8C)	0.3780	0.1079	0.3795
C(1)	0.1925 (3)	0.2267 (3)	0.1505 (4)	HCp(9A)	0.1748	0.1164	0.4965
O(1)	0.1610 (3)	0.2144 (2)	0.0745 (3)	HCp(9B)	0.1284	0.1621	0.4749
C(2)	0.2697 (6)	0.2557 (4)	0.3186 (6)	HCp(9C)	0.2135	0.1707	0.4956
O(2)	0.3006 (7)	0.2681 (3)	0.3950 (7)	HCp(10A)	0.0339	0.0866	0.3082
Cp(1)	0.1856 (4)	0.0704 (3)	0.2207 (4)	HCp(10B)	0.0441	0.1346	0.2383
Cp(2)	0.2625 (4)	0.0644 (3)	0.2514 (4)	HCp(10C)	0.0494	0.1555	0.3334
Cp(3)	0.2668 (4)	0.0903 (3)	0.3463 (4)	HCp(16A)	0.1753	0.3345	0.0000
Cp(4)	0.1928 (4)	0.1121 (3)	0.3743 (4)	HCp(16B)	0.2256	0.4015	−0.0132
Cp(5)	0.1428 (4)	0.1001 (3)	0.2965 (4)	HCp(16C)	0.1438	0.4123	−0.0013
Cp(6)	0.1524 (5)	0.0453 (4)	0.1251 (5)	HCp(17A)	0.3508	0.4770	0.1160
Cp(7)	0.3259 (5)	0.0275 (4)	0.1982 (6)	HCp(17B)	0.3426	0.4055	0.0649
Cp(8)	0.3380 (5)	0.0889 (4)	0.4094 (6)	HCp(17C)	0.3810	0.4071	0.1572
Cp(9)	0.1718 (7)	0.1392 (5)	0.4726 (6)	HCp(18A)	0.3169	0.4913	0.3580
Cp(10)	0.0586 (5)	0.1152 (4)	0.2941 (7)	HCp(18B)	0.3579	0.4189	0.3315
Cp(11)	0.1962 (4)	0.3924 (3)	0.1241 (4)	HCp(18C)	0.3014	0.4152	0.4032
Cp(12)	0.2662 (3)	0.4113 (3)	0.1713 (4)	HCp(19A)	0.1608	0.3765	0.4361
Cp(13)	0.2520 (4)	0.4157 (3)	0.2714 (4)	HCp(19B)	0.0861	0.3842	0.3756
Cp(14)	0.1725 (4)	0.4008 (3)	0.2863 (4)	HCp(19C)	0.1238	0.4491	0.3982
Cp(15)	0.1394 (3)	0.3860 (3)	0.1950 (4)	HCp(20A)	0.0425	0.3618	0.2216
Cp(16)	0.1847 (4)	0.3834 (3)	0.0181 (4)	HCp(20B)	0.0523	0.3254	0.1399
Cp(17)	0.3421 (4)	0.4284 (3)	0.1240 (5)	HCp(20C)	0.0319	0.4086	0.1490
Cp(18)	0.3095 (4)	0.4382 (3)	0.3480 (5)	H(13A)	0.0454	0.1444	−0.3664
Cp(19)	0.1348 (5)	0.4014 (4)	0.3816 (5)	H(13B)	0.0147	0.0718	−0.3823
Cp(20)	0.0558 (4)	0.3678 (4)	0.1737 (6)	H(14A)	0.0695	0.0762	−0.2366
Na	−0.0992 (1)	0.2490 (1)	−0.2355 (2)	H(14B)	−0.0130	0.0608	−0.2258
N(12)	−0.0686 (3)	0.1459 (2)	−0.3674 (3)	H(16A)	0.0716	0.1388	−0.0734
C(13)	0.0080 (4)	0.1132 (4)	−0.3469 (5)	H(16B)	0.0026	0.0951	−0.0799
C(14)	0.0221 (4)	0.0951 (4)	−0.2452 (5)	H(17A)	0.0124	0.2334	−0.0286
O(15)	0.0139 (2)	0.1587 (2)	−0.1898 (3)	H(17B)	−0.0143	0.1745	0.0286
C(16)	0.0202 (5)	0.1403 (5)	−0.0898 (5)	H(19A)	−0.1220	0.2342	0.0673
C(17)	−0.0153 (5)	0.1910 (5)	−0.0322 (5)	H(19B)	−0.1826	0.2392	0.0021
O(18)	−0.0902 (2)	0.2079 (2)	−0.0592 (3)	H(20A)	−0.0767	0.3405	0.0290
C(19)	−0.1324 (5)	0.2505 (4)	0.0070 (5)	H(20B)	−0.1546	0.3496	0.0466
C(20)	−0.1227 (5)	0.3282 (4)	0.0036 (5)	H(22A)	−0.0780	0.4531	−0.0460
N(21)	−0.1329 (3)	0.3629 (3)	−0.0883 (4)	H(22B)	−0.1061	0.4603	−0.1434
C(22)	−0.0829 (5)	0.4278 (4)	−0.1018 (5)	H(23A)	0.0177	0.3830	−0.0912
C(23)	−0.0079 (5)	0.4083 (4)	−0.1370 (6)	H(23B)	0.0206	0.4499	−0.1424
O(24)	−0.0069 (3)	0.3680 (2)	−0.2244 (3)	H(25A)	0.0042	0.4529	−0.3046
C(25)	−0.0238 (4)	0.4108 (4)	−0.3052 (6)	H(25B)	−0.0742	0.4231	−0.3069
C(26)	−0.0061 (4)	0.3694 (4)	−0.3917 (5)	H(26A)	0.0440	0.3578	−0.3917
O(27)	−0.0502 (3)	0.3027 (2)	−0.3937 (3)	H(26B)	−0.0180	0.3969	−0.4441
C(28)	−0.0258 (4)	0.2526 (4)	−0.4663 (5)	H(28A)	0.0259	0.2436	−0.4531
C(29)	−0.0709 (4)	0.1826 (3)	−0.4618 (4)	H(28B)	−0.0281	0.2779	−0.5231
C(30)	−0.1264 (4)	0.0873 (3)	−0.3625 (4)	H(29A)	−0.0572	0.1489	−0.5103
C(31)	−0.2057 (4)	0.1152 (4)	−0.3617 (5)	H(29B)	−0.1246	0.1923	−0.4774
O(32)	−0.2136 (2)	0.1650 (2)	−0.2825 (3)	H(30A)	−0.1168	0.0580	−0.3062
C(33)	−0.2866 (5)	0.2010 (5)	−0.2813 (7)	H(30B)	−0.1200	0.0530	−0.4102
C(34)	−0.2882 (5)	0.2641 (5)	−0.2308 (9)	H(31A)	−0.2421	0.0779	−0.3524
O(35)	−0.2313 (2)	0.3157 (2)	−0.2486 (4)	H(31B)	−0.2179	0.1402	−0.4157
C(36)	−0.2383 (4)	0.3846 (4)	−0.2000 (8)	H(33A)	−0.3227	0.1698	−0.2585
C(37)	−0.2124 (5)	0.3855 (4)	−0.1019 (6)	H(33B)	−0.3033	0.2106	−0.3415
HCp(6A)	0.1881	0.0449	0.0968	H(34A)	−0.2883	0.2544	−0.1662
HCp(6B)	0.1213	0.0824	0.1009	H(34B)	−0.3349	0.2873	−0.2372
HCp(6C)	0.1325	−0.0001	0.1297	H(36A)	−0.2875	0.4005	−0.2039
HCp(7A)	0.3344	−0.0198	0.1994	H(36B)	−0.2132	0.4203	−0.2333
HCp(7B)	0.3732	0.0510	0.2123	H(37A)	−0.2434	0.3561	−0.0674
HCp(7C)	0.3259	0.0427	0.1340	H(37B)	−0.2196	0.4313	−0.0777
HCp(8A)	0.3505	0.0442	0.4395				

B. Anisotropic Thermal Coefficients (×10⁵)

	β_{11}	β_{22}	β_{33}	β_{12}	β_{13}	β_{23}		β_{11}	β_{22}	β_{33}	β_{12}	β_{13}	β_{23}
Co(1)	354	194	525	−16	−60	27	N(12)	366	299	456	5	−23	18
Co(2)	358	195	535	−29	−117	34	C(13)	520	434	675	81	68	−37
C(1)	432	242	618	14	−36	2	C(14)	411	415	822	83	−10	92
O(1)	1036	301	714	−65	−399	−8	O(15)	429	519	509	170	−100	−32
C(2)	1392	248	1412	−137	−1084	150	C(16)	654	836	877	433	−254	−148
O(2)	3624	322	3211	−342	−3036	324	C(17)	575	961	661	229	−80	93
Cp(1)	425	197	512	−69	75	−21	O(18)	444	463	598	130	24	−17
Cp(2)	386	230	664	23	153	73	C(19)	792	491	700	1	318	71
Cp(3)	522	254	572	30	−79	66	C(20)	1017	502	740	151	178	−44
Cp(4)	555	248	494	44	113	3	N(21)	468	341	800	33	83	20
Cp(5)	310	247	839	15	146	58	C(22)	714	445	982	−65	−27	−125
Cp(6)	913	355	874	−173	−96	−44	C(23)	634	508	1095	−196	−142	−61

Table IV (*Continued*)

	β_{11}	β_{22}	β_{33}	β_{12}	β_{13}	β_{23}		β_{11}	β_{22}	β_{33}	β_{12}	β_{13}	β_{23}
Cp(7)	760	365	1309	145	546	169	O(24)	536	375	752	−44	−58	82
Cp(8)	828	461	1116	38	−407	247	C(25)	610	360	1095	−137	−69	105
Cp(9)	1508	580	848	237	352	−116	C(26)	670	426	825	−68	100	142
Cp(10)	599	420	1853	−20	206	130	O(27)	522	339	689	−53	65	37
Cp(11)	464	214	553	19	−102	50	C(28)	574	510	579	2	60	114
Cp(12)	356	210	619	−1	−81	35	C(29)	600	394	517	−13	21	−24
Cp(13)	479	202	546	−15	−173	28	C(30)	611	310	695	4	−71	−20
Cp(14)	494	197	577	5	33	35	C(31)	559	410	824	−196	−206	77
Cp(15)	284	276	800	−4	−129	−4	O(32)	302	527	999	16	−51	−100
Cp(16)	814	303	554	30	−279	62	C(33)	434	636	1895	−131	−14	−252
Cp(17)	527	309	1068	−35	28	38	C(34)	387	613	2841	72	150	−76
Cp(18)	776	267	897	−98	−370	−34	O(35)	328	460	1257	9	−1	9
Cp(19)	911	491	673	67	228	−10	C(36)	385	503	1978	218	92	150
Cp(20)	544	391	1469	75	−187	−28	C(37)	784	452	1106	186	204	−19
Na	312	335	581	−2	−3	11							

C. Root-Mean-Square Thermal Displacements (Å) of Selected Atoms along Their Principal Ellipsoidal Axes

	$\mu(1)$	$\mu(2)$	$\mu(3)$		$\mu(1)$	$\mu(2)$	$\mu(3)$		$\mu(1)$	$\mu(2)$	$\mu(3)$
Co(1)	0.18	0.21	0.25	C(1)	0.20	0.24	0.26	C(2)	0.19	0.20	0.57
Co(2)	0.18	0.20	0.26	O(1)	0.21	0.23	0.43	O(2)	0.21	0.22	0.92

[a] 2,2,2-crypt denotes $N(C_2H_4OC_2H_4OC_2H_4)_3N$. [b] The estimated standard deviations of the least significant figures are given in parentheses. [c] Anisotropic temperature factors of the form $\exp\{-[\beta_{11}h^2 + \beta_{22}k^2 + \beta_{33}l^2 + 2\beta_{12}hk + 2\beta_{13}hl + 2\beta_{23}kl]\}$ were used. [d] In the final full-matrix least-squares cycle performed on a HARRIS/7 computer only the positional parameters of the nonhydrogen atoms were varied. All anisotropic and isotropic thermal parameters as well as the positional parameters of the hydrogen atoms were assigned as fixed contributors obtained from a previous converged block-diagonal refinement. Idealized hydrogen positions (at distances of 0.90 Å from their attached carbon atoms) were not varied during least-squares refinement but were recalculated after every other cycle so as to take into account the shifts in the positions of the carbon atoms. The arbitrarily assigned thermal parameters of 6.0 $Å^2$ for all hydrogen atoms were held constant.

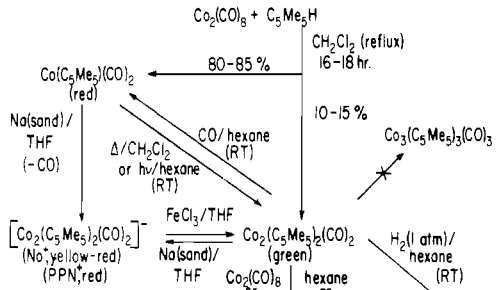

Figure 8. Reaction scheme for the $[Co_2(\eta^5\text{-}C_5Me_5)_2(\mu\text{-}CO)_2]^n$ series (n = 0, 1−). A comparison with the reaction scheme in Figure 1 for the corresponding unsubstituted-cyclopentadienyl cobalt dimers reveals similarities and differences in chemical behavior.

tributed to the asymmetrical stretching mode. The absence of the corresponding symmetric mode in the solid-state spectrum of the neutral dimer is presumably due to the $Co_2(CO)_2$ core approximating centrosymmetric symmetry, which forbids IR activity of this latter mode. The appearance of only one IR band in solution for both complexes may be ascribed to the existence of a planar centrosymmetric $Co_2(CO)_2$ core in solution, which in the absence of crystal packing forces is stabilized by the multiple Co–Co bonding.

Synthesis, Characterization, and Reactivity of $Co_2(\eta^5\text{-}C_5Me_5)_2(\mu\text{-}CO)_2$. The synthesis of the $Co_2(\eta^5\text{-}C_5Me_5)_2(\mu\text{-}CO)_2$ neutral dimer has been accomplished by three different routes (Figure 8). The first method[1,10] utilized the slow oxidation of the $[Co_2(\eta^5\text{-}C_5Me_5)_2(\mu\text{-}CO)_2]^-$ monoanion with anhydrous $FeCl_3$ in high yield. However, the overall yield of the neutral dimer from $Co(\eta^5\text{-}C_5Me_5)(CO)_2$ by this route is limited by the reasonable yields (50–60%) obtained in the preparation of the monoanion. The second method employed the thermolysis of $Co(\eta^5\text{-}C_5Me_5)(CO)_2$ to prepare $Co_2(\eta^5\text{-}C_5Me_5)_2(\mu\text{-}CO)_2$. Ginsburg and Dahl[1] noted the formation of the neutral dimer (10% yield) as a byproduct in the preparation of $Co(\eta^5\text{-}C_5Me_5)(CO)_2$ by the reaction of C_5Me_5H and $Co_2(CO)_8$ in CH_2Cl_2, while Cotton, Kaska, and co-workers[8] obtained the dimer (62% yield) by refluxing (pentamethylcyclopentadienyl)cobalt dicarbonyl in toluene. This method is directly analogous to the preparation by King and Efraty[33] of $Mo_2(\eta^5\text{-}C_5Me_5)_2(CO)_4$, which contains a Mo–Mo triple bond; in this case the direct reaction of acetylpentamethylcyclopentadiene with $M(CO)_6$ (M = Cr, Mo, W) yields the dimeric species. In fact, King[34] predicted that pentamethylcyclopentadienyl complexes could be an entry to the direct synthesis of unsaturated metal clusters of first- and second-row transition metals. Unfortunately, both of the above-mentioned syntheses require time-consuming purification steps. The third and most convenient method of synthesis of this neutral cobalt dimer is accomplished by the photolysis of $Co(\eta^5\text{-}C_5Me_5)(CO)_2$ under a continuous purge of nitrogen to facilitate removal of carbon monoxide. The photolysis can be carried out either in a Pyrex glass apparatus with THF as the solvent (4–5 days), or in a quartz apparatus with hexane or toluene as the solvent (6–8 h). Yields are typically of the order of 90–95% of pure microcrystalline dimer. When the quartz photolysis apparatus is used, care must be taken to stop the photolysis immediately after the formation of the dimer in order to prevent the formation of decomposition products such as $Co_3(\eta^5\text{-}C_5Me_5)_2(CO)_3(\mu\text{-}CO)(\mu_3\text{-}CCH_3)$, which was formed[24] after an extended period of irradiation. This method is analogous to that of Lee and Brintzinger,[3] who observed $Co_2(\eta^5\text{-}C_5H_5)_2(\mu\text{-}CO)_2$ as an intermediate in the photolysis of $Co(\eta^5\text{-}C_5H_5)(CO)_2$.

The properties of $Co_2(\eta^5\text{-}C_5Me_5)_2(\mu\text{-}CO)_2$ (Figure 8) are somewhat different from those (Figure 1) of $Co_2(\eta^5\text{-}C_5H_5)_2(\mu\text{-}CO)_2$.[3,35] The latter compound, prepared either by the oxidation of the $[Co_2(\eta^5\text{-}C_5H_5)_2(\mu\text{-}CO)_2]^-$ monoanion or by the photochemical reaction of $Co(\eta^5\text{-}C_5H_5)(CO)_2$, is unstable in solution and decomposes to the $Co_3(\eta^5\text{-}C_5H_5)_3(\mu\text{-}CO)_2(\mu_3\text{-}CO)$ trimer.[3,9] It is also characterized by a tendency to undergo asymmetric cleavage, both in a mass spectrometer

(33) (a) King, R. B.; Efraty, A. *J. Am. Chem. Soc.* **1971**, *93*, 4950–4952. (b) *Ibid.* **1972**, *94*, 3773–3779.
(34) King, R. B. *Coord. Chem. Rev.* **1976**, *20*, 155–169.
(35) Vollhardt, K. P. C.; Bercaw, J. E.; Bergman, R. G. *J. Organomet. Chem.* **1975**, *97*, 283–297.

Table V. Interatomic Distances, Bond Angles, and Torsional Angles for $[Na(2,2,2\text{-crypt})]^+[Co_2(\eta^5\text{-}C_5Me_5)_2(\mu\text{-}CO)_2]^-$

A. Intraanion Distances (Å)

Co(1)–Co(2)	2.372 (1)	Co(1)–Cp(1c)[a]	1.736	Cp(1)–Cp(6)	1.510 (8)
C(1)···C(2)	2.727 (9)	Co(2)–Cp(2c)[a]	1.736	Cp(2)–Cp(7)	1.491 (8)
Co(1)–C(1)	1.820 (6)	Co(1)–Cp(1)	2.110 (5)	Cp(3)–Cp(8)	1.504 (9)
Co(2)–C(1)	1.834 (6)	Co(1)–Cp(2)	2.126 (5)	Cp(4)–Cp(9)	1.500 (9)
	1.827 (av)	Co(1)–Cp(3)	2.109 (6)	Cp(5)–Cp(10)	1.487 (9)
Co(1)···O(1)	2.849 (4)	Co(1)–Cp(4)	2.094 (6)		1.498 (av)
Co(2)···O(1)	2.854 (4)	Co(1)–Cp(5)	2.086 (6)	Cp(11)–Cp(12)	1.414 (8)
	2.851 (av)		2.105 (av)	Cp(12)–Cp(13)	1.418 (7)
Co(1)–C(2)	1.800 (7)	Co(2)–Cp(11)	2.111 (5)	Cp(13)–Cp(14)	1.424 (8)
Co(2)–C(2)	1.792 (7)	Co(2)–Cp(12)	2.136 (5)	Cp(14)–Cp(15)	1.412 (8)
	1.796 (av)	Co(2)–Cp(13)	2.120 (5)	Cp(15)–Cp(11)	1.410 (8)
Co(1)···O(2)	2.809 (6)	Co(2)–Cp(14)	2.114 (6)		1.416 (av)
Co(2)···O(2)	2.808 (6)	Co(2)–Cp(15)	2.082 (6)	Cp(11)–Cp(16)	1.494 (8)
	2.808 (av)		2.113 (av)	Cp(12)–Cp(17)	1.514 (8)
Co(1)–O(1)	1.204 (6)	Cp(1)–Cp(2)	1.400 (8)	Cp(13)–Cp(18)	1.505 (8)
C(2)–O(2)	1.204 (8)	Cp(2)–Cp(3)	1.401 (8)	Cp(14)–Cp(19)	1.486 (8)
		Cp(3)–Cp(4)	1.404 (8)	Cp(15)–Cp(20)	1.512 (9)
		Cp(4)–Cp(5)	1.395 (8)		1.502 (av)
		Cp(5)–Cp(1)	1.403 (7)		
			1.401 (av)		

B. Intraanion Angles (Deg)

Co(1)–C(1)–Co(2)	81.0 (2)	Cp(6)–Cp(1)–Cp(5)	125.1 (6)
Co(1)–C(2)–Co(2)	82.6 (3)	Cp(6)–Cp(1)–Cp(2)	126.6 (6)
	81.8 (av)	Cp(7)–Cp(2)–Cp(1)	126.2 (6)
C(1)–Co(1)–C(2)	97.8 (3)	Cp(7)–Cp(2)–Cp(3)	125.7 (7)
C(1)–Co(2)–C(2)	97.5 (3)	Cp(8)–Cp(3)–Cp(2)	125.3 (7)
	97.6 (av)	Cp(8)–Cp(3)–Cp(4)	126.2 (6)
Co(1)–C(1)–O(1)	140.0 (5)	Cp(9)–Cp(4)–Cp(3)	125.3 (7)
Co(1)–C(2)–O(2)	137.7 (6)	Cp(9)–Cp(4)–Cp(5)	126.8 (7)
Co(2)–C(1)–O(1)	138.9 (5)	Cp(10)–Cp(5)–Cp(4)	126.2 (6)
Co(2)–C(2)–O(2)	138.3 (6)	Cp(10)–Cp(5)–Cp(1)	125.7 (7)
	138.7 (av)		125.9 (av)
Cp(1c)–Co(1)–Co(2)	167.4	Cp(11)–Cp(12)–Cp(13)	108.0 (5)
Cp(2c)–Co(2)–Co(1)	168.1	Cp(12)–Cp(13)–Cp(14)	108.4 (5)
	167.8 (av)	Cp(13)–Cp(14)–Cp(15)	106.7 (5)
Cp(1c)–Co(1)–C(1)	131.6	Cp(14)–Cp(15)–Cp(11)	109.4 (5)
Cp(1c)–Co(1)–C(2)	130.0	Cp(15)–Cp(11)–Cp(12)	107.5 (5)
Cp(2c)–Co(2)–C(1)	130.7		108.0 (av)
Cp(2c)–Co(2)–C(2)	131.2	Cp(16)–Cp(11)–Cp(15)	126.6 (6)
	130.9 (av)	Cp(16)–Cp(11)–Cp(12)	125.9 (6)
Cp(1)–Cp(2)–Cp(3)	107.5 (5)	Cp(17)–Cp(12)–Cp(11)	126.5 (5)
Cp(2)–Cp(3)–Cp(4)	108.4 (6)	Cp(17)–Cp(12)–Cp(13)	125.4 (5)
Cp(3)–Cp(4)–Cp(5)	107.7 (5)	Cp(18)–Cp(13)–Cp(12)	125.9 (6)
Cp(4)–Cp(5)–Cp(1)	108.1 (5)	Cp(18)–Cp(13)–Cp(14)	125.5 (6)
Cp(5)–Cp(1)–Cp(2)	108.2 (5)	Cp(19)–Cp(14)–Cp(13)	124.7 (6)
	108.0 (av)	Cp(19)–Cp(14)–Cp(15)	128.6 (6)
		Cp(20)–Cp(15)–Cp(14)	126.5 (6)
		Cp(20)–Cp(15)–Cp(11)	124.1 (6)
			126.0 (av)

C. Intracation Distances (Å)

Na–N(12)	2.665 (5)	O(15)–C(14)	1.385 (7)	O(15)···O(18)	2.728 (6)
Na–O(15)	2.618 (4)	O(15)–C(16)	1.432 (8)	O(24)···O(27)	2.726 (6)
Na–O(18)	2.562 (4)	O(18)–C(17)	1.383 (8)	O(32)···O(35)	2.763 (7)
Na–N(21)	2.957 (6)	O(18)–C(19)	1.410 (8)	O(15)···N(12)	2.846 (6)
Na–O(24)	2.674 (5)	O(24)–C(23)	1.414 (8)	O(27)···N(12)	2.856 (6)
Na–O(27)	2.558 (4)	O(24)–C(25)	1.387 (8)	O(32)···N(12)	2.819 (6)
Na–O(32)	2.571 (5)	O(27)–C(26)	1.421 (8)	O(18)···N(21)	2.905 (6)
Na–O(35)	2.591 (5)	O(27)–C(28)	1.421 (7)	O(24)···N(21)	2.914 (7)
N(12)–C(13)	1.477 (8)	O(32)–C(31)	1.427 (8)	O(35)···N(21)	2.914 (7)
N(12)–C(29)	1.470 (7)	O(32)–C(33)	1.423 (9)		
N(12)–C(30)	1.456 (8)	O(35)–C(34)	1.380 (10)		
N(21)–C(20)	1.430 (8)	O(35)–C(36)	1.415 (9)		
N(21)–C(22)	1.467 (9)	C(13)–C(14)	1.469 (9)		
N(21)–C(37)	1.448 (9)	C(16)–C(17)	1.364 (10)		
		C(19)–C(20)	1.407 (9)		
		C(22)–C(23)	1.441 (10)		
		C(25)–C(26)	1.451 (9)		
		C(28)–C(29)	1.481 (9)		
		C(30)–C(31)	1.465 (9)		
		C(33)–C(34)	1.334 (12)		
		C(36)–C(37)	1.430 (11)		

D. Torsional Angles (Deg) in the $[Na(2,2,2\text{-crypt})]^+$ Cation

N(12)–C(13)–C(14)–O(15)	122.1	C(26)–C(25)–O(24)–C(23)	168.3
C(13)–C(14)–O(15)–C(16)	−174.5	C(25)–O(24)–C(23)–C(22)	−105.5
C(14)–O(15)–C(16)–C(17)	156.3	O(24)–C(23)–C(22)–N(21)	−123.2

Table V (*Continued*)

O(15)-C(16)-C(17)-O(18)	129.7	N(12)-C(30)-C(31)-O(32)	−122.9
C(16)-C(17)-O(18)-C(19)	−170.2	C(30)-C(31)-O(32)-C(33)	−174.0
C(17)-O(18)-C(19)-C(20)	−95.9	C(31)-O(32)-C(33)-C(34)	−158.6
O(18)-C(19)-C(20)-N(21)	128.1	O(32)-C(33)-C(34)-O(35)	−130.7
N(12)-C(29)-C(28)-O(27)	124.6	C(33)-C(34)-O(35)-C(36)	−174.8
C(29)-C(28)-O(27)-C(26)	−177.1	C(34)-O(35)-C(36)-C(37)	99.8
C(28)-O(27)-C(26)-C(25)	−168.9	O(35)-C(36)-C(37)-N(21)	−123.2
O(27)-C(26)-C(25)-O(24)	−120.9		

E. Intraionic and Interionic Nonbonding Distances (Å)

Cp(6)···C(1)	3.347 (9)	Cp(16)···O(1)	3.162 (8)	C(16)···O(1)	3.58 (1)
Cp(6)···O(1)	3.119 (8)	Cp(16)···C(1)	3.364 (6)	C(17)···O(1)	3.41 (1)
Cp(8)···C(2)	3.451 (10)	Cp(18)···O(2)	3.127 (8)		
Cp(8)···O(2)	3.286 (10)	Cp(18)···C(2)	3.373 (9)		
Cp(9)···O(2)	3.405 (15)	HCp(16A)···O(1)	2.40 (1)		
HCp(6B)···O(1)	2.50 (1)	HCp(18C)···O(2)	2.64 (1)		
HCp(8B)···O(2)	2.78 (1)				
HCp(9C)···O(2)	2.71 (1)				

[a] Cp(1c) refers to the centroid of the cyclopentadienyl ring comprised of Cp(1), Cp(2), Cp(3), Cp(4), and Cp(5), while Cp(2c) refers to the centroid of the cyclopentadienyl ring composed of Cp(11), Cp(12), Cp(13), Cp(14), and Cp(15).

Table VII. Atomic Parameters for $Co_2(\eta^5\text{-}C_5Me_5)_2(\mu\text{-}CO)_2$[a]

A. Positional Parameters

	10^4x	10^4y	10^4z		10^4x	10^4y	10^4z
Co(1)	7928.4 (13)	7370.6 (10)	1084.2 (9)	H(6C)	7021	5184	1831
Co(2)	10179.8 (13)	7356.1 (11)	746.4 (9)	H(7A)	5220	7229	−946
O(1)	9545 (9)	5777 (6)	1732 (7)	H(7B)	3951	6569	−432
O(2)	8642 (9)	9007 (7)	248 (7)	H(7C)	5657	6056	−535
C(1)	9321 (10)	6485 (9)	1346 (8)	H(8A)	4210	8813	−163
C(2)	8825 (11)	8257 (8)	546 (9)	H(8B)	6006	8881	−468
Cp(1)	6317 (11)	6551 (7)	1371 (8)	H(8C)	5635	9544	−541
Cp(2)	5809 (11)	7082 (8)	573 (8)	H(9A)	7465	8823	2936
Cp(3)	5939 (12)	8017 (9)	790 (9)	H(9B)	7550	9355	2014
Cp(4)	6612 (12)	8073 (8)	1745 (9)	H(9C)	6083	9285	2341
Cp(5)	6800 (11)	7167 (9)	2099 (8)	H(10A)	7952	7352	3365
Cp(6)	6274 (13)	5563 (8)	1430 (9)	H(10B)	6517	6800	3338
Cp(7)	5134 (12)	6726 (9)	−357 (8)	H(10C)	7889	6315	3022
Cp(8)	5453 (12)	8795 (9)	181 (9)	H(16A)	11770	5228	1290
Cp(9)	6926 (14)	8933 (10)	2286 (10)	H(16B)	11253	5153	99
Cp(10)	7371 (13)	6878 (11)	3084 (9)	H(16C)	13048	5255	620
Cp(11)	11868 (11)	6532 (9)	587 (8)	H(17A)	12623	7474	2765
Cp(12)	12322 (11)	7170 (10)	1284 (8)	H(17B)	13991	6878	2430
Cp(13)	12059 (12)	8061 (9)	924 (9)	H(17C)	12671	6381	2515
Cp(14)	11516 (12)	7978 (8)	−40 (8)	H(18A)	11984	9572	1227
Cp(15)	11350 (10)	7027 (7)	−245 (8)	H(18B)	12224	9069	2086
Cp(16)	11984 (12)	5526 (9)	652 (8)	H(18C)	13385	9228	1622
Cp(17)	12955 (13)	6937 (10)	2258 (9)	H(19A)	12176	8859	−1004
Cp(18)	12377 (14)	8929 (10)	1418 (9)	H(19B)	10982	9373	−283
Cp(19)	11202 (12)	8755 (8)	−697 (8)	H(19C)	10216	8546	−1222
Cp(20)	10837 (11)	6622 (8)	−1197 (7)	H(20A)	10297	7360	−1525
H(6A)[b]	6255	5145	900	H(20B)	12075	6417	−1285
H(6B)	5509	5210	1635	H(20C)	10056	6039	−905

B. Anisotropic Thermal Parameters (X10^4)[c]

	β_{11}	β_{22}	β_{33}	β_{12}	β_{13}	β_{23}		β_{11}	β_{22}	β_{33}	β_{12}	β_{13}	β_{23}
Co(1)	48.0 (17)	38.4 (9)	42.6 (9)	−0.4 (10)	20.5 (10)	−3.0 (7)	Cp(8)	107 (18)	63 (8)	79 (9)	41 (10)	47 (11)	32 (7)
Co(2)	48.1 (18)	45.8 (10)	42.7 (9)	−2.8 (10)	23.6 (10)	−1.8 (7)	Cp(9)	145 (21)	85 (10)	88 (11)	17 (12)	38 (12)	33 (8)
O(1)	103 (12)	70 (6)	114 (8)	32 (7)	69 (8)	45 (6)	Cp(10)	121 (19)	121 (12)	51 (8)	−8 (12)	32 (11)	6 (8)
O(2)	125 (13)	61 (7)	152 (9)	13 (7)	101 (9)	39 (6)	Cp(11)	55 (14)	71 (9)	32 (7)	10 (9)	26 (8)	2 (7)
C(1)	41 (13)	55 (8)	58 (7)	2 (8)	38 (8)	4 (6)	Cp(12)	46 (13)	100 (11)	31 (7)	7 (10)	15 (8)	−2 (7)
C(2)	55 (15)	39 (7)	84 (9)	0 (8)	49 (10)	6 (6)	Cp(13)	54 (14)	57 (8)	57 (9)	−15 (9)	32 (9)	−8 (7)
Cp(1)	66 (14)	34 (7)	58 (8)	−6 (8)	27 (9)	−2 (6)	Cp(14)	75 (15)	52 (8)	41 (7)	−8 (8)	19 (8)	−4 (6)
Cp(2)	59 (14)	45 (7)	57 (8)	−1 (8)	36 (8)	−5 (6)	Cp(15)	40 (12)	38 (6)	51 (8)	−12 (7)	19 (8)	−11 (5)
Cp(3)	68 (15)	62 (8)	51 (8)	12 (9)	26 (9)	7 (6)	Cp(16)	110 (17)	60 (8)	52 (8)	28 (9)	36 (9)	14 (6)
Cp(4)	70 (15)	43 (7)	66 (9)	−2 (8)	26 (9)	−17 (7)	Cp(17)	83 (16)	116 (11)	47 (7)	15 (12)	23 (9)	1 (8)
Cp(5)	51 (13)	77 (9)	35 (7)	4 (9)	31 (8)	1 (6)	Cp(18)	157 (22)	85 (10)	82 (10)	−69 (12)	56 (12)	−44 (8)
Cp(6)	125 (19)	43 (8)	106 (12)	−5 (9)	65 (12)	12 (7)	Cp(19)	106 (18)	55 (7)	60 (9)	−6 (9)	25 (10)	8 (6)
Cp(7)	86 (16)	93 (10)	43 (7)	−12 (11)	8 (9)	−15 (7)	Cp(20)	89 (16)	61 (8)	37 (7)	7 (9)	12 (9)	0 (5)

[a] Estimated standard deviations are given in parentheses. [b] Fixed isotropic temperature factors of 6.0 Å^2 were used for the hydrogen atoms. The idealized coordinates obtained for the hydrogen atoms were also not varied in the least-squares refinement. [c] Anisotropic temperature factors are of the form $\exp[-\beta_{11}h^2 + \beta_{22}k^2 + \beta_{33}l^2 + 2\beta_{12}hk + 2\beta_{13}hl + 2\beta_{23}kl)]$.

and in solution. On the other hand, $Co_2(\eta^5\text{-}C_5Me_5)_2(\mu\text{-}CO)_2$ in much more thermally stable, though still very air-sensitive. This neutral dimer does not form in solution a triangular cobalt cluster with three bridging carbonyl ligands in accord with our

Table VIII. Interatomic Distances and Bond Angles for $Co_2(\eta^5\text{-}C_5Me_5)_2(\mu\text{-}CO)_2$

A. Intramolecular Distances (Å) Averaged under Assumed C_{2v} Symmetry for the $Co_2(CO)_2$ Core

Co(1)–Co(2)	2.338 (2)	Co(1)–Cp(1c)[a]	1.688	Cp(1)–Cp(6)	1.458 (16)
C(1)···C(2)	2.868 (18)	Co(2)–Cp(2c)[a]	1.706	Cp(2)–Cp(7)	1.501 (16)
Co(1)–C(1)	1.860 (12)	Co(1)–Cp(1)	2.086 (10)	Cp(3)–Cp(8)	1.478 (15)
Co(2)–C(2)	1.856 (11)	Co(1)–Cp(2)	2.083 (11)	Cp(4)–Cp(9)	1.499 (16)
	1.858 (av)	Co(1)–Cp(3)	2.114 (11)	Cp(5)–Cp(10)	1.520 (16)
Co(1)···O(1)	2.876 (9)	Co(1)–Cp(4)	2.046 (11)		1.491 (av)
Co(2)···O(1)	2.883 (9)	Co(1)–Cp(5)	2.064 (10)	Cp(11)–Cp(12)	1.404 (16)
	2.880 (av)		2.079 (av)	Cp(12)–Cp(13)	1.421 (17)
Co(1)–C(2)	1.841 (12)	Co(2)–Cp(11)	2.090 (11)	Cp(13)–Cp(14)	1.431 (15)
Co(2)–C(2)	1.847 (12)	Co(2)–Cp(12)	2.085 (11)	Cp(14)–Cp(15)	1.436 (15)
	1.844 (av)	Co(2)–Cp(13)	2.066 (11)	Cp(15)–Cp(11)	1.436 (15)
Co(1)···O(2)	2.862 (9)	Co(2)–Cp(14)	2.126 (11)		1.426 (av)
Co(2)···O(2)	2.868 (9)	Co(2)–Cp(15)	2.097 (10)	Cp(11)–Cp(16)	1.487 (16)
	2.865 (av)		2.093 (av)	Cp(12)–Cp(17)	1.495 (16)
C(1)–O(1)	1.188 (13)	Cp(1)–Cp(2)	1.424 (15)	Cp(13)–Cp(18)	1.475 (17)
C(2)–O(2)	1.190 (13)	Cp(2)–Cp(3)	1.413 (16)	Cp(14)–Cp(19)	1.495 (15)
	1.189 (av)	Cp(3)–Cp(4)	1.441 (16)	Cp(15)–Cp(20)	1.526 (14)
		Cp(4)–Cp(5)	1.432 (16)		1.496 (av)
		Cp(5)–Cp(1)	1.419 (15)		
			1.426 (av)		

B. Intramolecular Angles (Deg) Averaged under Assumed C_{2v} Symmetry for the $Co_2(CO)_2$ Core

Co(1)–C(1)–Co(2)	78.0 (5)	Cp(1)–Cp(2)–Cp(3)	110.1 (11)	Cp(11)–Cp(12)–Cp(13)	109.4 (10)
Co(1)–C(2)–Co(2)	78.7 (5)	Cp(2)–Cp(3)–Cp(4)	106.5 (10)	Cp(12)–Cp(13)–Cp(14)	107.6 (10)
	78.4 (av)	Cp(3)–Cp(4)–Cp(5)	108.0 (10)	Cp(13)–Cp(14)–Cp(15)	107.4 (10)
C(1)–Co(1)–C(2)	101.6 (5)	Cp(4)–Cp(5)–Cp(1)	108.4 (10)	Cp(14)–Cp(15)–Cp(11)	107.9 (10)
C(1)–Co(2)–C(2)	101.5 (5)	Cp(5)–Cp(1)–Cp(2)	106.9 (10)	Cp(15)–Cp(11)–Cp(12)	107.5 (11)
	101.6 (av)		108.0 (av)		108.0 (av)
Co(1)–C(1)–O(1)	140.3 (8)	Cp(6)–Cp(1)–Cp(5)	126.9 (12)	Cp(16)–Cp(11)–Cp(15)	124.7 (11)
Co(1)–C(2)–O(2)	140.6 (9)	Cp(6)–Cp(1)–Cp(2)	126.0 (12)	Cp(16)–Cp(11)–Cp(12)	127.6 (11)
Co(2)–C(1)–O(1)	141.6 (8)	Cp(7)–Cp(2)–Cp(1)	126.2 (11)	Cp(17)–Cp(12)–Cp(11)	124.7 (13)
Co(2)–C(2)–O(2)	140.6 (9)	Cp(7)–Cp(2)–Cp(3)	123.6 (11)	Cp(17)–Cp(12)–Cp(13)	125.8 (12)
	140.8 (av)	Cp(8)–Cp(3)–Cp(2)	127.8 (12)	Cp(18)–Cp(13)–Cp(12)	127.4 (12)
Cp(1c)–Co(1)–Co(2)	179.4	Cp(8)–Cp(3)–Cp(4)	125.8 (12)	Cp(18)–Cp(13)–Cp(14)	124.8 (12)
Cp(2c)–Co(2)–Co(1)	179.6	Cp(9)–Cp(4)–Cp(3)	125.5 (12)	Cp(19)–Cp(14)–Cp(13)	125.2 (11)
	179.5 (av)	Cp(9)–Cp(4)–Cp(5)	126.3 (12)	Cp(19)–Cp(14)–Cp(15)	127.5 (11)
Cp(1c)–Co(1)–C(1)	129.2	Cp(10)–Cp(5)–Cp(4)	127.7 (12)	Cp(20)–Cp(15)–Cp(14)	125.4 (11)
Cp(1c)–Co(1)–C(2)	129.1	Cp(10)–Cp(5)–Cp(1)	123.9 (13)	Cp(20)–Cp(15)–Cp(11)	126.5 (10)
Cp(2c)–Co(2)–C(1)	129.2		126.0 (av)		126.0 (av)
Cp(2c)–Co(2)–C(2)	129.1				
	129.2 (av)				

[a] Cp(1c) refers to the centroid of the cyclopentadienyl ring comprised of Cp(1), Cp(2), Cp(3), Cp(4), and Cp(5), while Cp(2c) refers to the centroid of the cyclopentadienyl ring composed of Cp(11), Cp(12), Cp(13), Cp(14), and Cp(15).

prejudice that the sterically bulky pentamethylcyclopentadienyl ligands along with three bridging carbonyls would inhibit such an oligomerization. Hence, steric constraints appear to play an important role in the chemistry of the pentamethylcyclopentadienyl metal clusters.

A mass spectrum of $Co_2(\eta^5\text{-}C_5Me_5)_2(\mu\text{-}CO)_2$ exhibits a parent ion peak at m/e 444 along with peaks assignable to $[Co(C_5Me_5)(CO)_2]^+$ and $[Co(C_5Me_5)(CO)]^+$. The tendency of methylated-cyclopentadienyl compounds, such as found for $Ni_2(\eta\text{-}C_5H_4Me)_2(\mu\text{-}CO)_2$[15] and $Cr_2(\eta^5\text{-}C_5Me_5)_2(CO)_4$,[36] to fragment into fulvene-type species is also observed here, with the peak assignable to the $[Co_2(C_5(CH_3)_4CH_2)_2]^+$ ion being the base peak in the mass spectrum.

The single infrared carbonyl absorption band observed at 1760 (hexane) and 1750 cm^{-1} (Nujol mull) for $Co_2(\eta^5\text{-}C_5Me_5)_2(\mu\text{-}CO)_2$ is consistent with a planar $Co_2(CO)_2$ core. The fact that this carbonyl frequency for the neutral pentamethylcyclopentadienyl dimer in hexane solution is 38 cm^{-1} lower than that of 1798 cm^{-1} for the corresponding unsubstituted-cyclopentadienyl neutral dimer, $Co_2(\eta^5\text{-}C_5H_5)_2(\mu\text{-}CO)_2$,[3] in petroleum ether may be attributed to the electron-rich C_5Me_5 ligands raising the dicobalt orbitals relative to those in the unsubstituted-cyclopentadienyl dimer and thereby giving rise to greater $d_\pi(Co) \rightarrow \pi^*(CO)$ back-bonding. A ^1H NMR spectrum of the neutral $Co_2(\eta^5\text{-}C_5Me_5)_2(\mu\text{-}CO)_2$ dimer exhibits a methyl resonance at δ 1.40, which indicates greater shielding than that found in the monomeric $Co(\eta^5\text{-}C_5Me_5)(CO)_2$, which has a methyl resonance at δ 1.92.

Experimental and Theoretical Analyses of the Electronic Structures of the Metal–Metal Multiple-Bonded $[Co_2(\eta^5\text{-}C_5R_5)_2(\mu\text{-}CO)_2]^n$ Series (n = 0, 1–). (a) The Pinhas–Hoffmann MO Model Applied to the Unpaired Electron in the $[Co_2(\eta^5\text{-}C_5H_5)_2(\mu\text{-}CO)_2]^-$ Monoanion and the Possible Alternative HOMO Assigned by Schore from ESR Measurements. In the course of their crystallographic investigation of $Co_2(\eta^5\text{-}C_5H_5)_2(\mu\text{-}NO)_2$ (which has a Co–Co BO of 1.0) and the paramagnetic $Co_2(\eta^5\text{-}C_5H_5)_2(\mu\text{-}CO)(\mu\text{-}NO)$ (which formally corresponds to a Co–Co BO of 1.5), Bernal et al.[11] noted that the metal–metal bond separations in these dimers as well as in the previously determined structures of the $Fe_2(\eta^5\text{-}C_5H_5)_2(\mu\text{-}NO)_2$ dimer[6,7] (Fe–Fe BO = 2.0) and the $[Co_2(\eta^5\text{-}C_5H_5)_2(\mu\text{-}CO)_2]^-$ monoanion[2] (Co–Co BO = 1.5) appeared to be invariant to formal bond order as calculated by the EAN rule (see Table X for a bond length comparison). Their work was largely responsible for a resulting comprehensive theoretical analysis by Pinhas and Hoffmann[14] involving calculations of Walsh-type diagrams in order to interrelate the planar vs. bent geometrical configurations as well as metal–metal distances in several classes of dibridged binuclear metal com-

(36) Efraty, A.; Huang, M. H. A.; Weston, C. A. *Inorg. Chem.* **1977**, *16*, 79–84.

Table X. Comparison of Mean Geometrical Parameters for $M_2(\eta^5\text{-}C_5R_5)_2(\mu\text{-}X)_2$-Type Cyclopentadienyl Metal Dimers Containing Only Bridging Carbonyl and/or Nitrosyl Ligands

dimer	ref	cryst site symm of dimer	idealized M_2E_2 geometry[a]	torsional angle of M_2E_2 core,[b] deg	M-M BO[c]	M-M, Å	M-E, Å	M-Cp(c),[d] Å	E-M-E', deg	M-E-M', deg
$Ni_2(\eta^5\text{-}C_5H_5)_2(\mu\text{-}CO)_2$	*i*	C_1-1	C_{2v} (bent)[e]	146, 139[e]	1.0	2.363 (9), 2.351 (9)[e]	1.861, 1.869[e]	1.751, 1.752[e]	95.3, 93.4[e]	78.8, 78.1[e]
$Ni_2(\eta^5\text{-}C_5H_4Me)_2(\mu\text{-}CO)_2$	*i*	C_{2h}-2/*m*	C_{2h} (planar)[f]	180	1.0	2.390 (1)	1.840, 1.889	1.745	100.3	79.7
$Co_2(\eta^5\text{-}C_5H_5)_2(\mu\text{-}NO)_2$	*j*	C_i-1	D_{2h} (planar)	180	1.0	2.372 (1)	1.825	1.724	98.9 (3)	81.1 (3)
$[PPN]^+[Co_2(\eta^5\text{-}C_5H_5)_2(\mu\text{-}CO)_2]^-$	*k*	C_i-1	D_{2h} (planar)[n]	180	1.5	2.372 (2), 2.359 (2)[n]	1.82 (2)[n]	*h*	98.5 (5)[n]	81.2 (5)[n]
$[AsPh_4]^+[Co_2(\eta^5\text{-}C_5H_5)_2(\mu\text{-}CO)_2]^-$	*l*	C_i-1	D_{2h} (planar)	180	1.5	2.364 (2)	1.815	1.736	98.7 (4)	81.3 (4)
$[Na(2,2,2\text{-crypt})]^+[Co_2(\eta^5\text{-}C_5Me_5)_2(\mu\text{-}CO)_2]^-$	*l*	C_1-1	C_{2v} (bent)	168	1.5	2.372 (1)	1.827	1.736	97.6 (3)	81.0 (2)
$Co_2(\eta^5\text{-}C_5H_5)_2(\mu\text{-}CO)(\mu\text{-}NO)$	*j*	C_i-1	C_{2v} (planar)[g]	180	1.5	2.370 (1)	1.829 (7)	1.723	99.3 (2)	80.7 (2)
$Co_2(\eta^5\text{-}C_5Me_5)_2(\mu\text{-}CO)_2$	*l*	C_1-1	C_{2v} (bent)	176	2.0	2.338 (2)	1.851	1.697	101.6 (5)	78.4 (5)
$Fe_2(\eta^5\text{-}C_5H_5)_2(\mu\text{-}NO)_2$	*m*	C_i-1	D_{2h} (planar)	180	2.0	2.326 (4)	1.768 (9)	*h*	97.7 (4)	82.3 (4)

[a] E denotes either C or N. [b] Torsional angle between two planes in the M_2E_2 core each formed by the bridging E atoms and one M atom. [c] Calculated in accord with the EAN rule. [d] Denotes the centroid of the cyclopentadienyl ring. [e] Mean values are given for the molecular parameters of the two crystallographically independent molecules. [f] The M_2C_2 core ideally conforms to C_{2h}-2/*m* symmetry due to the two centrosymmetrically related carbonyl ligands being asymmetrically coordinated by 0.049 Å to the two nickel atoms. This bridging carbonyl asymmetry is attributed to electronic effects involving the particular disposition of the C_5H_4Me ligands. [g] The centrosymmetric site symmetry necessitates that the bridging CO and NO ligands are crystallographically disordered, corresponding to an average planar C_{2v} geometry for a given $Co_2(CO)(NO)$ fragment. [h] Data not available. [i] Reference 15. [j] Reference 11. [k] Reference 2. [l] This work. [m] Reference 7. [n] Mean values are given for the two crystallographically independent half-dimers of the monoanion.

Figure 9. Schematic representation of four frontier MO's of $[Co_2(\eta^5\text{-}C_5R_5)_2(\mu\text{-}CO)_2]^n$ (n = 0, 1−) illustrating under assumed C_{2v}-*m2m* symmetry the orbital topology for the $Co_2(CO)_2$ core together with their presumed qualitative energy-level ordering for the monoanion.

plexes including the above carbonyl- and nitrosyl-bridged cyclopentadienylmetal dimers. A planar configuration is illustrated schematically in Figure 9 for the $Co_2(CO)_2$ core of the $[Co_2(\eta^5\text{-}C_5H_5)_2(\mu\text{-}CO)_2]^-$ monoanion.

The atomic coordinate system (x, y, z) presented here for the $Co_2(CO)_2$ core is the same as that utilized by Byers and Dahl[25] for the planar $Co(CO)_2$ core in the mononuclear $Co(\eta^5\text{-}C_5Me_5)(CO)_2$ complex but different from that (x', y', z') utilized by Pinhas and Hoffmann[14] (for which $x' = x$, $y' = z$, $z' = y$) and that (x'', y'', z'') later used by Schore[18] (for which $x'' = y$, $y'' = x$, $z'' = z$) for the $[Co_2(\eta^5\text{-}C_5H_5)_2(\mu\text{-}CO)_2]^-$ monoanion; our particular choice of atomic coordinate system is based upon a comparative analysis (vide infra) between the two equivalent $Co\text{–}C_5Me_5$ interactions in the corresponding neutral dimer and that in the $Co(\eta^5\text{-}C_5Me_5)(CO)_2$ monomer.

In the case of the $[Co_2(\eta^5\text{-}C_5H_5)_2(\mu\text{-}CO)_2]^n$ series (n = 0, 1−, 2−), Pinhas and Hoffmann[14] showed that the presence or absence of a puckering of the $Co_2(CO)_2$ core together with the changes in the calculated Co–Co bond lengths upon a variation in formal Co–Co bond order (resulting from either oxidation of the monoanion to the neutral parent molecule or reduction to the (as yet) unknown dianion) primarily involve three frontier MO's of representations b_2, a_2, and a_1 under C_{2v} symmetry. These three MO's as well as the fourth one of b_1 representation are constructed from linear combinations of the two individual π-like orbitals on each $(\eta^5\text{-}C_5H_5)Co$ moiety to give in-plane dimetal π_{xz}-bonding and dimetal π^*_{xz}-antibonding symmetry orbitals (SO's) as well as out-of-plane dimetal π_{yz}-bonding and dimetal π^*_{yz}-antibonding SO's for the resulting $(\eta^5\text{-}C_5H_5)_2Co_2$ unit.

Four resulting frontier MO's are then formed from these four dimetal SO's by appropriate combinations with the carbonyl frontier symmetry orbitals (viz., dicarbonyl combinations of either the valence lone-pair 5σ(CO) or π^*(CO) SO's).[37] Figure 9 gives a schematic representation of these four frontier MO's illustrating under C_{2v}-*m2m* symmetry (where the twofold axis in our coordinate system is in the y direction) the nature of the presumed dominant orbital character for only the $Co_2(CO)_2$ core.

Whereas the out-of-plane π^*_{yz} (b_2) SO cannot interact by symmetry with any of the carbonyl frontier symmetry orbitals (viz., combinations of either the valence lone-pair 5σ(CO) or π^*(CO) SO's), the other three $(\eta^5\text{-}C_5H_5)_2Co_2$ SO's interact substantially with the corresponding dicarbonyl SO's of the same representations. Pinhas and Hoffmann[14] assumed that the in-plane $\pi_{xz}(b_1)$ SO is raised to a high energy as part of an antibonding $[\pi_{xz}\text{–}5\sigma(CO)_u]^*$ MO from its interaction with the lower energy *ungerade* 5σ(CO) SO (b_1). In contrast, the in-plane π^*_{xz} SO (a_2) is stabilized by its strong back-bonding

(37) See: (a) Fenske, R. F. *Pure Appl. Chem.* **1971**, *27*, 61–71. (b) Fenske, R. F.; DeKock, R. L. *Inorg. Chem.* **1970**, *9*, 1053–1060.

interaction with the empty, high-energy, in-plane π^*_z(CO) SO (a_2) of *gerade* symmetry, while the out-of-plane π_{yz} SO (a_1) is also stabilized by its back-bonding interaction with the empty, high-energy, out-of-plane π^*_y(CO) SO (a_1) of *ungerade* symmetry. On the basis of the Hoffmann–Pinhas ordering of the energy levels for these frontier MO's (Figure 9), the unpaired electron in the $[Co_2(\eta^5\text{-}C_5H_5)_2(\mu\text{-}CO)_2]^-$ monoanion (and likewise in the pentamethylcyclopentadienyl analogue) resides in the out-of-plane π^*_{yz} MO (b_2), which is strongly antibonding with respect to the two metal atoms. Pinhas and Hoffmann[14] predicted that the removal of an electron from this molecular orbital in the formation the neutral dicobalt dimer from its monoanion would result in a shortening of the Co–Co bond distance by ~0.08 Å. However, the Co–Co distances determined from the crystallographic studies of the $[Co_2(\eta^5\text{-}C_5H_5)_2(\mu\text{-}CO)_2]^-$ monoanion (Co–Co BO = 1.5) and $Co_2(\eta^5\text{-}C_5H_5)_2(\mu\text{-}CO)(\mu\text{-}NO)$ (Co–Co BO = 1.5) are virtually identical with that found in $Co_2(\eta^5\text{-}C_5H_5)_2(\mu\text{-}NO)_2$ (Co–Co BO = 1.0). Hoffmann and Pinhas[14] had no explanation of the presumed discrepancy between the calculated and observed distances. They speculated that perhaps some MO other than the b_2 one was occupied in the case of the above nitrosyl dimer.

A subsequent qualitative analysis of the electronic structure in the $[Co_2(\eta^5\text{-}C_5H_5)_2(\mu\text{-}CO)_2]^-$ monoanion was reported by Schore[18] on the basis of his preparation and characterization by ESR and infrared measurements of the Na^+ salts of five (substituted-cyclopentadienyl)cobalt carbonyl dimeric monoanions, $[Co_2(\eta^5\text{-}C_5R_5)_2(\mu\text{-}CO)_2]^-$ (where $C_5R_5 = C_5Me_5$, $C_5H_4CO_2Me$, $C_5H_4SiPh_2Me$, $C_5H_4SiMe_3$, or $C_5H_4CH_2CO_2Me$). For all of these dimeric radicals g_{iso} and g_1 were found to be 2.08 ± 0.01 and 2.18 ± 0.01, respectively, while a_{iso} and a_1 varied over a 10% range, thereby indicating variations in the spin density of the cobalt atoms in the above series. From qualitative MO considerations analogous to the above description, Schore[18] concluded that the ESR spectral data for each monoanion are consistent with the placement of the unpaired electron in either the out-of-plane π^*_{yz} MO (b_2) or the in-plane antibonding $[\pi_{xz}\text{–}5\sigma(CO)_\mu]^*$ MO (b_1). He pointed out that from the available experimental evidence no distinction between these two possibilities could be made at that time.

(b) Bond Length and Spectral Analysis of the $[Co_2(\eta^5\text{-}C_5Me_5)_2(\mu\text{-}CO)_2]^n$ Series (n = 0, 1−) and Resulting Bonding Implications. A comparative analysis of the crystallographic results of this investigation clearly indicates that the unpaired electron in the $[Co_2(\eta^5\text{-}C_5Me_5)_2(\mu\text{-}CO)_2]^-$ monoanion occupies the out-of-plane π^*_{yz} MO (b_2), in agreement with the theoretical prediction of Pinhas and Hoffmann.[14] This conclusion is based upon the observed bond length changes in the $Co_2(CO)_2$ core upon a removal of the unpaired electron from the monoanion to form the neutral dicobalt molecule. A *decrease* of 0.034 Å in the Co–Co bond length is accompanied by an *increase* of 0.024 Å in the mean Co–CO bond length. These opposite changes are totally inconsistent with the unpaired electron being in the in-plane, antibonding $[\pi_{xz}\text{–}5\sigma(CO)_\mu]^*$ MO (b_1) in that this MO is bonding between the two cobalt atoms but antibonding between the cobalt and carbonyl ligands. Hence, the removal of an electron from this HOMO would be expected to produce an increase in the Co–Co distance along with a decrease in the Co–CO bond lengths.

In contrast, a removal of the unpaired electron from the out-of-plane π^*_{yz} HOMO (b_2), which is strongly antibonding between the two metal atoms, would be expected to give rise to a significantly shorter Co–Co distance. The much smaller observed decrease of 0.034 Å relative to that of 0.08 Å predicted by Pinhas and Hoffmann[14] may be readily ascribed to the significant bond length increase in the Co–CO bonds (upon oxidation of the monoanion), which in being much stronger than the metal–metal interactions are the dominant factor in apparently opposing any decrease in the Co–Co distance. The fact that the imposed planar symmetry of the π^*_{yz} HOMO (b_2) precludes any carbonyl ligand orbital character points to the increase in the Co–CO bond lengths (upon oxidation of the monoanion to the neutral parent) being an indirect consequence of the loss of negative charge, which in turn lowers the metal AO's relative to the π^*(CO) SO's and thereby decreases the π back-bonding between the cobalt and carbonyl ligands. In other words, the lower energy in-plane π^*_{xz} SO (a_2) is less stabilized by its smaller back-bonding interaction with the higher energy, in-plane $\pi^*_z(CO)_g$SO (a_2), and likewise the lower energy out-of-plane π_{yz} SO (a_1) is also less stabilized by its smaller back-bonding interaction with the higher energy, out-of-plane $\pi^*_y(CO)_\mu$ SO (a_1). It is noteworthy that this charge effect is also consistent with the observed carbonyl IR frequency of 1670 cm^{-1} for the monoanion in THF solution being 80 cm^{-1} less than that of 1750 cm^{-1} for the neutral dimer in THF solution.

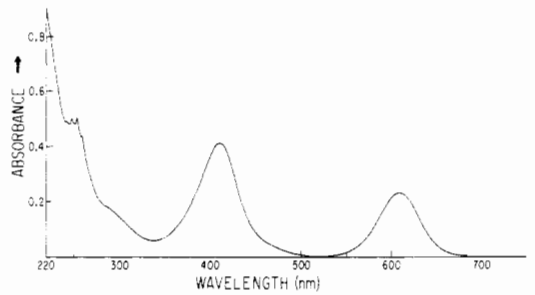

Figure 10. The UV-visible spectrum of $Co_2(\eta^5\text{-}C_5Me_5)_2(\mu\text{-}CO)_2$ recorded in hexane solution from 220 to 750 μm. The two intense absorptions centered at 610 and 410 nm with molar extinction coefficients of 1.0×10^4 and 2.1×10^4 L mol^{-1} cm^{-1}, respectively, have been tentatively assigned to the $a_2 \rightarrow b_2$ and $a_1 \rightarrow b_2$ electronic transitions.

The UV–visible spectrum (Figure 10) of the neutral $Co_2(\eta^5\text{-}C_5Me_5)_2(\mu\text{-}CO)_2$ dimer exhibits two prominent absorption bands at 610 and 410 nm with molar extinction coefficients of 1.0×10^4 and 2.1×10^4 L mol^{-1} cm^{-1}, respectively. In accordance with the Hoffmann–Pinhas energy level diagram,[14] these two low-energy bands may be tentatively assigned to the $a_2 \rightarrow b_2$ and $a_1 \rightarrow b_2$ transitions.

(c) Comparative Bond Length Analysis of the Co–C_5Me_5 Interactions in the Neutral Dimer with Those in $Co(\eta^5\text{-}C_5Me_5)(CO)_2$ and Resulting Bonding Implications. A close examination of the geometrical differences between the Co–(C_5Me_5) fragments of the neutral $[Co_2(\eta^5\text{-}C_5Me_5)_2(\mu\text{-}CO)_2]$ dimer and $Co(\eta^5\text{-}C_5Me_5)(CO)_2$ molecule provides additional bond length evidence that the LUMO in the neutral dimer and HOMO in its reduced monoanion is indeed the out-of-plane π^*_{yz} MO (b_2). These arguments are based upon the significant differences in both the corresponding Co–C(ring) and C(ring)–C(ring) bond lengths found between the neutral dimer and $Co(\eta^5\text{-}C_5Me_5)(CO)_2$, which have analogously oriented C_5Me_5 rings relative to the planar cobalt dicarbonyl fragments. A relatively precise crystallographic analysis of the latter molecule (Figure 11) by Byers and Dahl[25] provided convincing evidence for a statistically significant and theoretically meaningful distortion of the pentamethylcyclopentadienyl ring from fivefold symmetry due to its noncylindrical bonding interaction with a sterically innocent, planar $Co(CO)_2$ fragment. The C_5Me_5 ring is symmetrically disposed with respect to the planar $Co(CO)_2$ fragment such that the entire molecule experimentally conforms to a C_s-m geometry with the mirror plane bisecting both the C_5Me_5 ligand and OC–Co–CO bond angle. The symmetrically deformed C(ring)–C(ring) configuration consists of two mirror-related, adjacent intermediate C(11)–C(12) and C(11)–C(15) bonds of 1.414 (6) and 1.407

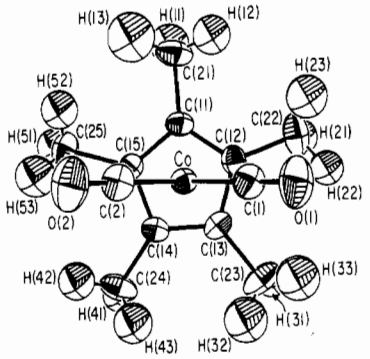

Figure 11. View of the molecular configuration of $Co(\eta^5\text{-}C_5Me_5)(CO)_2$.[25] The pseudobilateral mirror plane symmetry of the entire molecule is apparent. A comparative bond length analysis of the $Co\text{–}C_5Me_5$(ring) and C(ring)–C(ring) interactions in this molecule with those in the neutral $Co_2(\eta^5\text{-}C_5Me_5)_2(\mu\text{-}CO)_2$ dimer provides experimental evidence for the LUMO in the neutral dimer being the out-of-plane b_2 MO.

(6) Å, respectively, separated from one shorter C(13)–C(14) bond of 1.392 (6) Å by two mirror-related, longer C(12)–C(13) and C(14)–C(15) bonds of 1.445 (6) and 1.447 (6) Å, respectively. The C_5Me_5 ring was also found to possess a small but marked distortion from planarity by a folding about the C(12)···C(15) line, which is reflected in the equivalent Co–C(12) and Co–C(15) distances of 2.074 (4) and 2.062 (4) Å, respectively, being significantly shorter than the Co–C(11) distance of 2.102 (4) Å and the equivalent Co–C(13) and Co–C(14) distances of 2.101 (4) and 2.105 (4) Å, respectively. This particular ring deformation from a regular pentagonal geometry toward an "allyl–ene" geometry was attributed to a resulting localized distribution of p_π electron density on the C_5Me_5 ring due mainly to a breakdown of the doubly degenerate e_1 ring orbital degeneracy (Figure 12) by its interaction with a planar d^8 Co(I) dicarbonyl moiety, which does not possess cylindrical symmetry. On the basis of the same Cartesian coordinate system as that chosen for the cobalt dimers, the z axis is directed along the $Co\text{–}C_5Me_5$(centroid) while the x and y axes are directed within and perpendicular to the planar $Co(CO)_2^+$ fragment. From Figure 12 it follows that the resulting nondegenerate in-plane, empty d_{xz} and out-of-plane, filled d_{yz} Co(I) AO's extensively interact with the lower energy filled e_1^+ and e_1^- ring component SO's, respectively, to produce bonding and antibonding in-plane e_1^+(ring)–d_{xz}(Co) combinations and bonding and antibonding out-of-plane e_1^-(ring)–d_{yz}(Co) combinations. Since the three in-plane bonding and out-of-plane bonding and antibonding combinations are occupied and only the highest energy, in-plane antibonding $[e_1^+(\text{ring})\text{–}d_{xz}(\text{Co})]^*$ combination is unoccupied, the prime "net" electron-donor $e_1(\text{ring})\rightarrow d_\pi$(cobalt) interaction involves the e_1^+ diolefin ring component with the in-plane d_{xz} AO. Hence, the observed ring distortion reflects primarily the difference between depleted e_1^+ charge density relative to the e_1^- charge density on the ring. The observed longer Co–C(11), Co–C(13), and Co–C(14) bond lengths relative to the Co–C(12) and Co–C(15) bond lengths also reflect this resulting charge asymmetry due to "net" in-plane e_1^+(ring)–d_{xz}(Co) bonding involving principally the C(12) and C(15) ring atoms.

In complete contrast, the neutral $Co_2(\eta^5\text{-}C_5Me_5)_2(\mu\text{-}CO)_2$ dimer, which closely conforms to a molecular C_{2v}-$m2m$ symmetry with the two eclipsed C_5Me_5 rings each disposed to the $Co_2(CO)_2$ core in an analogous fashion to that in $Co(\eta^5\text{-}C_5Me_5)(CO)_2$, shows no evidence of either any C_5Me_5 ring distortion or the particular Co–C(ring) bond length pattern determined for the $Co(\eta^5\text{-}C_5Me_5)(CO)_2$ molecule. Instead, the observed distances (Table XI) are completely consistent with the LUMO in the neutral dimer being the out-of-plane

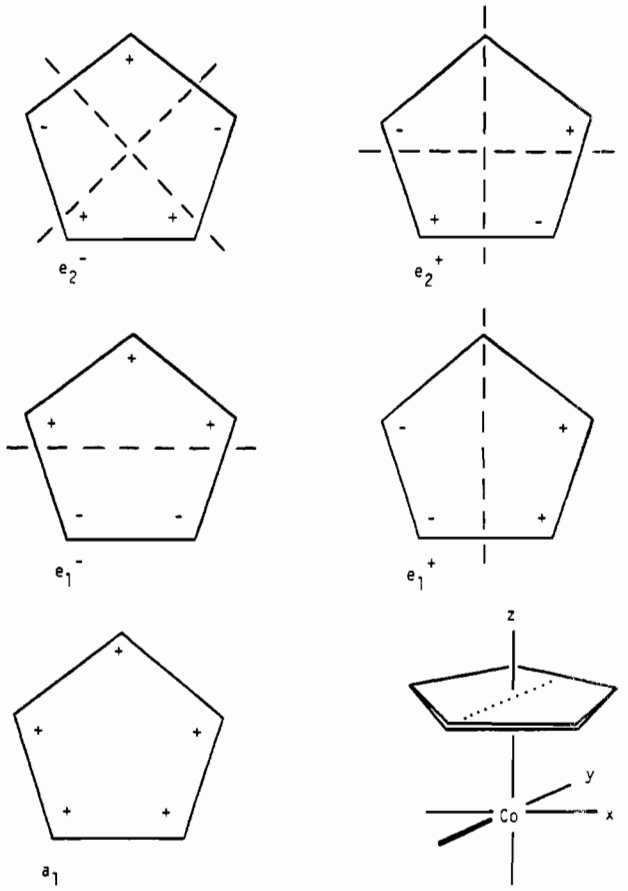

Figure 12. The five p_π ring symmetry orbitals (SO's) of the $C_5Me_5^-$ monoanion (under assumed C_{5v} symmetry) (nodal planes denoted by dashed lines). Under the indicated coordinate system in which the planar $Co(CO)_2$ fragment or corresponding planar $Co_2(CO)_2$ core lies in the xz plane, the predominant $Co\text{–}C_5Me_5$(ring) interactions involve the in-plane d_{xz}(Co)–e_1^+(ring) and out-of-plane d_{yz}(Co)–e_1^-(ring) π combinations.[25] In the case of the $Co(\eta^5\text{-}C_5Me_5)(CO)_2$ molecule, the observed C_5Me_5 ring distortion toward an "allyl–ene" geometry upon coordination to the $Co(CO)_2$ fragment results from the in-plane *bonding* $[d_{xz}(\text{Co})\text{–}e_1^+(\text{ring})]$ combination being filled but the corresponding in-plane *antibonding* $[d_{xz}(\text{Co})\text{–}e_1^+(\text{ring})]^*$ combination being empty, whereas both the out-of-plane *bonding* and *antibonding* $d_{yz}(\text{Co})\text{–}e_1^-(\text{ring})$ combinations are occupied.[25] In the case of the neutral $Co_2(\eta^5\text{-}C_5Me_5)_2(\mu\text{-}CO)_2$ dimer, for which each C_5Me_5 ring is simiarly disposed relative to the planar $Co_2(CO)_2$ core, the absence of an "allyl–ene" distortion of each C_5Me_5 ring and the distinctly different $Co\text{–}C_5Me_5$(ring) bond length pattern from that in the $Co(\eta^5\text{-}C_5Me_5)(CO)_2$ molecule (see Table XI) are completely consistent with the LUMO in the neutral dimer being the *out-of-plane* π^*_{yz} MO (b_2), which from energetic considerations must have considerable *antibonding* $d_{yz}(\text{Co})\text{–}e_1^-(\text{ring})$ orbital character.

π^*_{yz} MO (b_2), which from energetic considerations must have considerable antibonding $[e_1^-(\text{ring})\text{–}d_{yz}(\text{Co})]^*$ orbital character. The fact that this b_2 MO is *unoccupied* in the neutral dimer in contradistinction to the corresponding out-of-plane *antibonding* $[e_1^-(\text{ring})\text{–}d_{yz}(\text{Co})]^*$ MO (which also by symmetry can possess bonding $d_{yz}(\text{Co})\text{–}\pi^*_y(\text{CO})$ orbital character) of the $Co(\eta^5\text{-}C_5Me_5)(CO)_2$ molecule being *filled* should result in a "net" bonding $e_1(\text{ring})\rightarrow d_\pi(\text{Co})$ interaction in the neutral dimer involving both the in-plane $e^+(\text{ring})\rightarrow d_{xz}(\text{Co})$ and out-of-plane $e_1^-(\text{ring})\rightarrow d_{yz}(\text{Co})$ components. This predicted bonding difference is supported by the neutral dimer exhibiting under C_{2v}-$m2m$ symmetry three corresponding, independent sets of C(ring)–C(ring) bonds with *equivalent* mean values of 1.427, 1.427, and 1.424 Å, respectively (Table XI). Thus, the C_5Me_5 rings in the neutral dimer adhere to fivefold symmetry within experimental error. Furthermore, the three mean Co–C(ring) distances in the neutral dimer (which correspond

Table XI. Comparison of C(ring)–C(ring) and Co–C(ring) Bond Distances (Å) of $Co(\eta^5\text{-}C_5Me_5)(CO)_2$ with Corresponding Distances of $Co_2(\eta^5\text{-}C_5Me_5)_2(\mu\text{-}CO)_2$

C(11)–C(12)	1.414 (6)	1.413 (16)
C(11)–C(15)	1.407 (6)	1.436 (15)
	1.410 (av)	1.424 (15)
		1.436 (15)
		1.427 (av)
C(12)–C(13)	1.445 (6)	1.441 (16)
C(14)–C(15)	1.447 (6)	1.404 (16)
	1.446 (av)	1.419 (15)
		1.431 (15)
		1.424 (av)
C(13)–C(14)	1.392 (6)	1.432 (16)
		1.421 (17)
		1.427 (av)
Co–C(11)	2.102 (4)	2.083 (11)
		2.097 (11)
		2.090 (av)
Co–C(12)	2.072 (4)	2.114 (11)
Co–C(15)	2.062 (4)	2.090 (11)
	2.067 (av)	2.086 (10)
		2.126 (11)
		2.104 (av)
Co–C(13)	2.101 (4)	2.046 (11)
Co–C(14)	2.105 (4)	2.085 (11)
	2.103 (av)	2.064 (10)
		2.066 (11)
		2.065 (av)

to the Co–C(11) distance, the two equivalent Co–C(12) and Co–C(15) distances, and the two equivalent Co–C(13) and Co–C(14) distances in $Co(\eta^5\text{-}C_5Me_5)(CO)_2$ are 2.090, 2.104, and 2.065 Å, respectively. This intermediate–longer–shorter Co–C(ring) bond length pattern is opposite to the corresponding longer–shorter–longer Co–C(ring) bond length pattern previously given for the $Co(\eta^5\text{-}C_5Me_5)(CO)_2$ molecule. It is apparent that these distinct experimental variations in the corresponding C(ring)–C(ring) and Co–C(ring) distances between the $Co_2(\eta^5\text{-}C_5Me_5)_2(\mu\text{-}CO)_2$ and $Co(\eta^5\text{-}C_5Me_5)(CO)_2$ molecules point to the LUMO of the neutral dimer possessing a large component of highly antibonding *out-of-plane* $[e_1^-(\text{ring})\text{–}d_{yz}(\text{Co})]^*$ orbital character. This is consistent only if the LUMO in the neutral dimer and the HOMO in the corresponding monoanion corresponds to the out-of-plane b_2 MO. The considerable solid-state distortion of the $[Co_2(\eta^5\text{-}C_5Me_5)_2(\mu\text{-}CO)_2]^-$ monoanion in the $[Na(2,2,2\text{-crypt})]^+$ salt precludes a physically meaningful bond length comparison involving its nonperpendicular linkage of the two $Co(C_5Me_5)$ fragments with the nonplanar central $Co_2(CO)_2$ core.

(d) Analysis of the Isotropic Cobalt Coupling Constants for the Solution ESR Data of the $[Co_2(\eta^5\text{-}C_5R_5)_2(\mu\text{-}CO)_2]^-$ Monoanions (R = H, Me) and Resulting Stereochemical Bonding Implications. On the basis of his analysis of the electron spin resonance measurements of the $[Co_2(\eta^5\text{-}C_5H_5)_2(\mu\text{-}CO)_2]^-$ monoanion and the five substituted ring derivatives (vide supra) in THF at 25 °C, Schore[18] indicated that the isotropic cobalt hyperfine coupling constant value of $|a_{iso}| = 44.0 \pm 0.1$ G obtained for the $[Co_2(\eta^5\text{-}C_5Me_5)_2(\mu\text{-}CO)_2]^-$ monoanion is unusual in being significantly smaller (instead of larger) than the corresponding value of $|a_{iso}| = 47.3 \pm 0.1$ G for the $[Co_2(\eta^5\text{-}C_5H_5)_2(\mu\text{-}CO)_2]^-$ monoanion. However, it is our current belief that these experimental values are consistent with smaller (instead of larger) cobalt orbital character being expected for the HOMO possessing the unpaired electron in the pentamethylcyclopentadienyl dimeric monoanion relative to that in the unsubstituted-cyclopentadienyl dimeric monoanion (vide infra). Our prejudice is based upon the following qualitative considerations relating the ESR solution data at room temperature for these monoanions to their electronic structures.

The isotropic contact term in the hyperfine interaction of a cobalt nucleus ($I = {}^7/_2$ for ^{59}Co: 100% abundance) in a cobalt complex with an unpaired electron contained in a cobalt d AO has been ascribed[38] to the spin polarization of the inner s electrons. It also has been found[38] that such an interaction for cobalt complexes gives rise to a *negative* isotropic coupling constant. Since the observed 15-line ESR spectrum[1,2,10,18] of each of these dimeric monoanions in THF is characteristic of a hyperfine interaction of the unpaired electron with both ^{59}Co nuclei, it follows that the isotropic hyperfine coupling constant for the electron delocalized in a MO over both equivalent cobalt atoms will be half that for an electron localized in a d orbital on only one cobalt atom. Hence, in this case it is necessary to compare the values of $2a_{iso} = -88.0$ G for the $[Co_2(\eta^5\text{-}C_5Me_5)_2(\mu\text{-}CO)_2]^-$ monoanion and $2a_{iso} = -94.6$ G for the $[Co_2(\eta^5\text{-}C_5H_5)_2(\mu\text{-}CO)_2]^-$ monoanion with values of a_{iso} for complexes containing a single cobalt atom. These values compare favorably with those of −94.7 G obtained for $3d^7$ Co(II) doped in a MgO host lattice[39] and $3a_{iso} = -93$ G for $Co_3(CO)_9(\mu_3\text{-}S)$[40] in which the unpaired electron is delocalized over the three equivalent cobalt atoms in an antibonding in-plane tricobalt MO of nondegenerate a_2 representation under C_{3v} symmetry. The fact that the unpaired electron in each of the above two compounds is essentially localized in a d orbital on each cobalt atom indicates that the unpaired electron in each dimeric monoanion resides in a MO with primarily Co 3d AO character (and little if any Co 4s AO character). This observation is completely consistent with the unpaired electron in each monoanion occupying the out-of-plane π^*_{yz} MO of b_2 representation, which by symmetry cannot possess any Co 4s AO character.

Qualitative symmetry arguments support our premise that the out-of-plane π^*_{yz} HOMO (b_2) in the $[Co_2(\eta^5\text{-}C_5Me_5)_2(\mu\text{-}CO)_2]^-$ monoanion should contain greater pentamethylcyclopentadienyl orbital character (and hence less cobalt orbital character) compared to that for the corresponding π^*_{yz} HOMO in the $[Co_2(\eta^5\text{-}C_5H_5)_2(\mu\text{-}CO)_2]^-$ monoanion. From an energetic viewpoint, the more electron-donating C_5Me_5 ligands will raise the p_π ring SO levels relative to the 3d Co levels such that the lower energy, filled allyl–ene e_1^- ring component[25] (which under localized C_s-m symmetry at each cobalt atom is no longer degenerate with the diolefin e_1^+ ring component) is drawn closer in energy to the out-of-plane d_{yz} Co AO. The net effect would be a greater mixing of these orbitals such that the resulting π^*_{yz} HOMO would have greater antibonding C_5Me_5 orbital character. This predicted greater ligand character for the π^*_{yz} HOMO of the $[Co_2(\eta^5\text{-}C_5Me_5)_2(\mu\text{-}CO)_2]^-$ monoanion relative to that for the corresponding π^*_{yz} HOMO of the $[Co_2(\eta^5\text{-}C_5H_5)_2(\mu\text{-}CO)_2]^-$ monoanion is in harmony with a significantly lower ^{59}Co isotropic coupling constant magnitude of 44.0 ± 0.1 G for the solution ESR spectrum of the $[Co_2(\eta^5\text{-}C_5Me_5)_2(\mu\text{-}CO)_2]^-$ monoanion at 25 °C compared to that of 47.3 ± 0.1 G for the solution ESR spectrum of the $[Co_2(\eta^5\text{-}C_5H_5)_2(\mu\text{-}CO)_2]^-$ monoanion at 25 °C.

It is noteworthy that this conclusion is contradictory to the interpretation reached by Schore[18] from an analysis of the ESR measurements on glassy solutions of these two monoanions (together with the monosubstituted ring derivatives) in 2-methyltetrahydrofuran at 77 K. Factors possibly complicating a meaningful interpretation of the ESR data include (1) the lack of crystallographic structural data for the monosubstituted ring derivatives (e.g., the substituent on each ring may be

(38) McGarvey, B. R. *J. Phys. Chem.* **1967**, *71*, 51–67.
(39) Orton, J. W.; Auzins, P.; Wertz, J. E. *Phys. Rev.* **1960**, *119*, 1691–1692.
(40) (a) Strouse, C. E.; Dahl, L. F. *J. Am. Chem. Soc.* **1971**, *93*, 6032–6041. (b) Strouse, C. E.; Dahl, L. F. *Discuss. Faraday Soc.* **1969**, *No. 47*, 93–106.

oriented within the same plane containing the presumed planar $Co_2(CO)_2$ core as found[15] for each of the two centrosymmetrically related methylcyclopentadienyl rings in the $Ni_2(\eta^5\text{-}C_5H_4Me)_2(\mu\text{-}CO)_2$ dimer, which contains a planar $Ni_2(CO)_2$ core) and (2) the solid-state structure of the $[Co_2(\eta^5\text{-}C_5Me_5)_2(\mu\text{-}CO)_2]^-$ monoanion as the $[Na(2,2,2\text{-crypt})]^+$ salt exhibiting a large sterically induced distortion from planar C_{2v} symmetry in contrast to that found for its oxidized neutral parent. It is also evident that dilute single-crystal ESR studies of these monoanions doped in suitable diamagnetic hosts are highly desirable in order to reveal the full nature of the hyperfine interaction and thereby enable one to delineate more clearly a comparative bonding description of the unpaired electron in these dimeric radicals.

Acknowledgment. We are pleased to acknowledge support of this research by the National Science Foundation. We also wish to thank Mr. Mark A. Murphy and Mr. Don M. Washecheck for special experimental assistance.

Registry No. **1a**, 80127-68-0; **1b**, 58636-28-5; **3a**, 72271-22-8; **4**, 69657-52-9; $[Na]^+[Co_2(\eta^5\text{-}C_5H_5)_2(CO)_2]^-$, 62602-00-0; $[Na]^+[Co_2(\eta^5\text{-}C_5Me_5)_2(\mu\text{-}CO)_2]^-$, 71618-09-2; $Co(\eta^5\text{-}C_5H_5)(CO)_2$, 12078-25-0; $Co(\eta^5\text{-}C_5Me_5)(CO)_2$, 12129-77-0; $Co_2(CO)_8$, 10210-68-1.

Supplementary Material Available: Selected least-squares planes (Tables III, VI, and IX) together with a listing of the observed and calculated structure factor amplitudes for $[AsPh_4]^+[Co_2(\eta^5\text{-}C_5H_5)_2(\mu\text{-}CO)_2]^-$ and $Co_2(\eta^5\text{-}C_5Me_5)_2(\mu\text{-}CO)_2$ (25 pages). Ordering information is given on any current masthead page.

Contribution from the Department of Chemistry, University of Victoria, Victoria, British Columbia, Canada, V8W 2Y2

Coordination Chemistry of Bridging PR_2–O Ligands. Crystal and Molecular Structure of Bis(bis(dimethyl phosphito)difluoroborato)platinum(II), $[Pt((P(OMe)_2O)_2BF_2)_2]$

DAVID ERIC BERRY, GORDON WILLIAM BUSHNELL,* and KEITH ROGER DIXON

Received March 27, 1981

Crystals of $[Pt((P(OMe)_2O)_2BF_2)_2]$ are triclinic, space group $P\bar{1}$, with $a = 8.331$ (3) Å, $b = 9.794$ (4) Å, $c = 7.840$ (2) Å, $\alpha = 96.19$ (5)°, $\beta = 99.65$ (3)°, and $\gamma = 111.92$ (4)° for $Z = 1$. The structure shows square-planar platinum coordination and a chair conformation for the six-membered rings, $\overline{PtP(OMe)_2OB(F_2)OP(OMe)_2}$, such that the platinum and boron atoms lie respectively +0.623 and −0.543 Å on opposite sides of the mean plane defined by the P_2O_2 ring section. A reinvestigation by ^{31}P NMR does not support a previous claim for formation of tetraphosphorus macrocyclic ligands by hydrolysis of $[Pt((P(OMe)_2O)_2BF_2)_2]$.

Introduction

Several recent studies have shown that whenever PR_2O^- and PR_2OH ligands occupy mutually cis positions in a coordination complex, a hydrogen-bonded system, **1**, is formed.[1,2] Removal

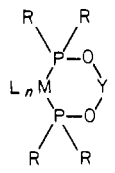

1, Y = H
2, Y = M'
3, Y = BF_2

of the hydrogen-bonded proton yields an anionic ligand, formally analogous to acetylacetonate, which can coordinate to a second metal[1,3,4] or be capped by groups such as BF_2.[1,3] Bimetallic complexes such as **2** are of considerable interest both as a means of holding two different metals in close proximity for catalysis studies and as a possible route to chain oligomers having different metal ions in specific ligand sites.[4]

The range of potential geometries for the six-membered ring systems in complexes **1**–**3** may be illustrated by the related bis(pyrazolyl)-bridged complexes where conformations range from the chair structure of $[(\eta^5\text{-}C_5H_5)_2Ti(\mu\text{-}C_3N_2H_3)]_2$[5] through planar for $[Ni(NO)(\mu\text{-}C_3N_2HMe_2)]_2$[6] to boat shaped in a cobalt(I) analogue.[7] For the present complexes the only available crystal structure determinations are for the hydrogen-bonded rings in $[Pd_2(\mu\text{-}NCS)_2((PPh_2O)_2H)_2]$[8] and $[Pd(S_2PMe_2)((PPh_2O)_2H)]$,[9] where it was not possible to locate the hydrogen atoms and hence establish the ring conformation. We have experienced difficulty in obtaining suitable crystals of several bimetallic systems of type **2** and hence decided to study initially the ring conformation in the known BF_2 capped complex $[Pt((P(OMe)_2O)_2BF_2)_2]$.[10] This system is also of interest because of earlier uncertainty as to whether $[Pt((P(OMe)_2O)_2BF_2)_2]$ or $[Pt((P(OMe)_2O)_2BF)_2]F_2$ is the correct formulation and because of the suggestion that hydrolysis leads to the macrocyclic complex, **4**, which may be converted to **5**

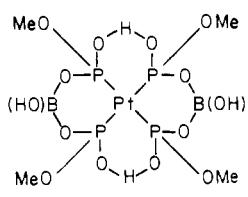

4

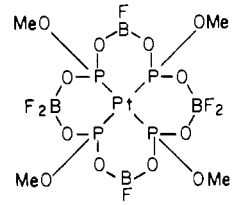

5

by further reaction with $BF_3{\cdot}OEt_2$.[10] Macrocyclic phosphorus ligands are very rare,[11] and we were therefore interested in obtaining definitive evidence for complexes **4** and **5**. We now

(1) Dixon, K. R.; Rattray, A. D. *Inorg. Chem.* **1977**, *16*, 209.
(2) Dixon, K. R.; Rattray, A. D. *Can. J. Chem.* **1971**, *49*, 3997.
(3) Roundhill, D. M.; Sperline, R. P.; Beaulieu, W. B. *Coord. Chem. Rev.* **1978**, *26*, 263 and references therein.
(4) Sperline, R. P.; Roundhill, D. M. *Inorg. Chem.* **1977**, *16*, 2612.
(5) Fieselmann, B. F.; Stucky, G. D. *Inorg. Chem.* **1978**, *17*, 2074.
(6) Chong, K. S.; Rettig, S. J.; Storr, A.; Trotter, J. *Can. J. Chem.* **1979**, *57*, 3090.
(7) Chong; K. S.; Rettig, S. J.; Storr, A.; Trotter, J. *Can. J. Chem.* **1979**, *57*, 3119.
(8) Naik, D. V.; Palenik, G. J.; Jacobson, S.; Carty, A. J. *J. Am. Chem. Soc.* **1974**, *96*, 2286.
(9) Cornock, M. C.; Gould, R. O.; Jones, C. L.; Stephenson, T. A. *J. Chem. Soc., Dalton Trans.* **1977**, 1307.
(10) Austin, T. E. Ph.D. Thesis, University of North Carolina, 1966.
(11) Deldonno, T. A.; Rosen, W. *J. Am. Chem. Soc.* **1977**, *99*, 8051. Kyba, E. P.; Hudson, C. W.; McPhaul, M. J.; John, A. M. *Ibid*, **1977**, *99*, 8054.

0020-1669/82/1321-0957$01.25/0